TIAGO ANDRÉ MOREIRA DA SILVA

THE ROLE OF SYNDECAN-4 IN GASTRIC CANCER CELL BIOLOGY

Dissertação de Candidatura ao grau de Mestre em Oncologia – Especialização em Oncologia Molecular submetida ao Instituto de Ciências Biomédicas de Abel Salazar da Universidade do Porto.

Orientadora - Doutora Ana Magalhães.

Afiliação - Grupo de Glicobiologia em Cancro, Instituto de Patologia e Imunologia Molecular da Universidade do Porto e Instituto de Investigação e Inovação em Saúde.

Co-orientador - Professor Doutor Celso Reis.

Categoria – Investigador Coordenador e Professor Auxiliar Convidado.

Afiliação - Grupo de Glicobiologia em Cancro, Instituto de Patologia e Imunologia Molecular da Universidade do Porto, Instituto de Investigação e Inovação em Saúde e Instituto de Ciências Biomédicas Abel Salazar da Universidade do Porto.

INSTITUTO DE CIÊNCIAS BIOMÉDICAS ABEL SALAZAR
UNIVERSIDADE DO PORTO

TÍTULO: The role of Syndecan-4 in gastric cancer cell biology.

Tese de Candidatura ao Grau de Mestre em Oncologia – Especialização em Oncologia Molecular submetida ao Instituto de Ciências Biomédicas Abel Salazar da Universidade do Porto.

AUTOR: Tiago André Moreira da Silva

CORREIO ELETRÓNICO: tiagoamsilva.01@gmail.com

1ªEDIÇÃO: Setembro de 2015

“*If you wish to be out front, then act as if you were behind*.” – Lao-Tzu, 6th Century B.C.

Agradecimentos

A elaboração deste trabalho e o findar deste ciclo não teria sido possível sem um conjunto de pessoas às quais tenho de agradecer verdadeiramente. Foi um ano algo difícil e exigente, mas que no fim se traduz não pelo alívio de ter acabado, mas sim por aquilo que tive o privilégio de aprender.

Começo por referir a pessoa mais importante para que, quer a minha confiança, quer a sensação de ter um trabalho com valor, nunca tenham resvalado ao longo deste ano. Essa pessoa é a Ana Magalhães, a minha orientadora. Independentemente do passar dos anos ou da distância que a vida se encarregue de colocar pelo meio, a Ana, mais do que ser a minha Brilhante Orientadora, será sempre uma Amiga de eleição e na qual valorizo todos os conselhos que me dá.

A minha passagem pelo IPATIMUP nunca teria sido possível se à 3 anos atrás a pessoa que teria o poder de decidir a aposta que estavam a fazer em mim, tivesse dito que não era possível. Refiro-me ao Dr. Celso. Obrigado pela oportunidade que me proporcionou e por toda a confiança que depositou em mim. Espero não o ter desiludido!

O trabalho que realizei foi sempre acompanhado de um fantástico e descontraído ambiente. Isso foi possível por estar inserido num Excelente grupo de pessoas que sempre me fizeram sentir bem e apoiado. Refiro-me ao grupo *Glycobiology in Cancer.* Destaco e agradeço verdadeiramente toda a ajuda e disponibilidade de três pessoas essenciais: Catarina Gomes, Joana Gomes e Daniela Freitas. Estiveram ao meu lado (com bastante paciência) a ensinar e a ajudar durante a ausência da Ana. Aos restantes membros, que merecem ser também destacados por serem pessoas excecionais (Ana Dias, Sandra, Márcia, Sara, Cíntia, Cláudia, Teresa, Henrique, Stefan e Tiago Oliveira) com os quais partilhei imensas gargalhadas, piadas e momentos de descontração, o meu profundo Obrigado. Dizem que o IPATIMUP é como uma família! Eu aprovo essa afirmação! Quer seja dentro do grupo a que pertenci, quer seja em contacto com todas as restantes pessoas do Instituto, Obrigado por me terem feito sentir sempre tão bem!

Devo destacar e agradecer a amabilidade de pessoas exteriores ao IPATIMUP que também contribuíram diretamente para que este trabalho tenha sido realizado. Ao Dr. Luís Pedro e ao Alexandre Ferreira (IPO Porto) o meu obrigado pela ajuda, cedência e posterior avaliação dos tecidos tumorais gástricos que recebemos do IPO Porto. Ao Dr. Guido David (KU Leuven, Bélgica) o meu agradecimento por nos ter cedido o anticorpo (8G3) para o estudo histoquímico que efetuei.

Por último, e não com menos destaque e importância que todas as pessoas acima referidas, devo o que sou, como sou e até onde cheguei aos pilares da minha vida. São eles: os meus Brilhantes pais, avós, irmão, sobrinha e cunhada. Obrigado por estarem sempre ao meu lado e apostarem, sem receios, no meu valor. Sem vocês não seria nada! Aos fantásticos Amigos que tenho o privilégio de ter ao meu lado e que sempre me acompanham pela vida, o meu sincero Obrigado!

Resumo

O cancro gástrico é um problema de saúde muito relevante com elevadas taxas de incidência e mortalidade a nível mundial. O comportamento maligno das células tumorais gástricas é determinado por vários mecanismos moleculares, sendo fundamental a interação entre importantes recetores membranares e o microambiente. O Syndecan-4 (SDC4) é um proteoglicano transmembranar ubiquamente expresso e com grande importância na adesão das células a componentes da matriz extracelular, deste modo regulando mecanismos de motilidade celular que são essenciais na carcinogénese gástrica. Adicionalmente, o SDC4 atua em cooperação com outros recetores membranares, nomeadamente as integrinas, na formação de contactos de adesão focais e na reorganização do citosqueleto. A interação das integrinas com o SDC4 é também importante para a sua reciclagem dinâmica e determina a sua localização subcelular.

Neste trabalho pretendemos compreender o papel funcional do SDC4 no comportamento das células de cancro gástrico e avaliar o seu envolvimento na tumorigénese gástrica. O silenciamento transiente do SDC4 foi realizado numa linha celular de cancro gástrico de forma a avaliar alterações na morfologia celular, bem como a expressão e localização celular da β1 integrina. Foram também efetuados ensaios funcionais de motilidade celular, migração e invasão, para avaliar o impacto do silenciamento do SDC4 nestes mecanismos associados a maior agressividade tumoral. Para validar a nossa abordagem *in vitro*, a expressão do SDC4 foi também avaliada numa série de diferentes tipos histológicos de carcinoma gástrico para investigar o potencial desta molécula como biomarcador no diagnóstico de cancro gástrico.

Os resultados obtidos demonstraram que o silenciamento transiente do SDC4 resultou num aumento da expressão da β1 integrina na membrana celular. As células de cancro gástrico com expressão silenciada de SDC4 adquiriram uma morfologia mais arredondada, menor capacidade de migração, mas maior capacidade de invadir. Observamos que a expressão de SDC4 é mais elevada nos carcinomas gástricos do tipo intestinal, sendo o SDC4 expresso na membrana apical e no citoplasma das células neoplásicas. Verificamos ainda expressão de SDC4 nas metástases linfáticas.

Este trabalho demonstra que o SDC4 desempenha um papel importante na biologia das células de carcinoma gástrico, determinando a sua morfologia e motilidade. Adicionalmente, a expressão de SDC4 em tumores gástricos humanos e respetivas metástases aponta para a importância deste proteoglicano na progressão do cancro gástrico e para a sua possível aplicação como biomarcador.

Abstract

Gastric cancer is a major health problem, with high incidence and mortality rates worldwide. The interaction between key membrane receptors and the surrounding cell microenvironment is one of the mechanisms underlying the malignant behaviour of gastric cancer. Syndecan-4 (SDC4) is an ubiquitously expressed transmembrane proteoglycan with key roles in cell adhesion to extracellular matrix components, thus regulating cell motility mechanisms which are crucial in gastric carcinogenesis. Additionally, SDC4 acts cooperatively with other cell surface receptors, namely integrins, to form focal adhesion contacts and modulate cytoskeleton structure. Such interplay is also important for integrin recycling dynamics, which directly influences integrins subcellular localization.

The present work aims to understand the role of SDC4 in gastric cancer cell behaviour and to evaluate the putative contribution of this molecule in gastric tumorigenesis. SDC4 transient knockdown was performed in a gastric cancer cell line in order to assess the role of this proteoglycan in cell morphology alterations and in β1 integrin expression levels and subcellular localization. Cell motility assays, such as migration and invasion, were also performed to assess the impact of SDC4 knockdown on such carcinogenic mechanisms. To validate this *in vitro* approach, SDC4 expression was assessed in a series of human gastric carcinoma clinical samples from distinct histological types, to assess the potential of this molecule as a novel biomarker for gastric cancer diagnosis.

Our results demonstrated that SDC4 transient knockdown cells have an increased β1 integrin expression at the cell membrane. Furthermore, the SDC4-silenced cancer cells acquired a more rounded morphology, with reduced migratory ability, but higher invasive capacity. Moreover, we observed that SDC4 expression was higher in intestinal-type gastric carcinomas and was preferentially located at the apical membrane and cytoplasm of neoplastic cells. Lymph node metastasis also presented SDC4 expression.

The present work demonstrates that SDC4 plays important roles in modulating gastric cancer cell biology and discloses its role in determining cancer cell morphology and motility. Moreover, SDC4 differential expression in human gastric cancer clinical samples strongly indicates this proteoglycan as a novel key player in gastric cancer progression, with putative biomarker applications.

Table of Contents

Figures Index

List of Abbreviations

GC	Gastric cancer
H. pylori	*Helicobacter pylori*
MALT	Mucosa-associated lymphoid tissue
ECM	Extracellular matrix
GlcNAc	N-acetylglucosamine
Asn	Asparagine
GalNAc	N-acetylgalactosamine
Ser	Serine
Thr	Threonine
GAG	Glycosaminoglycan
GlcA	Glucuronic acid
IdoA	Iduronic acid
HS	Heparan sulfate
CS	Chondroitin sulfate
DS	Dermatan sulfate
HSPG	Heparan sulfate proteoglycan
Xyl	Xylose
Gal	Galactose
NS	N-sulfated
NA	N-acetylated
PAPS	3’-phosphoadenosine-5’-phosphosulfate
SDC	Syndecan
ED	Extracellular domain
TM	Transmembrane domain
CD	Cytoplasmic domain
PKCα	Protein kinase Cα
siRNA	Small interfering RNA
PBS	Phosphate-buffered saline
BSA	Bovine serum albumin
WB	Western blot
qPCR	Quantitative Real-time PCR
siCTRL	Scrambled negative control siRNA
siSDC4	Combined siRNA ABC
IHC	Immunohistochemistry
WT	Wild-type

1. Introduction

Gastric cancer

Cancer is a leading public health issue worldwide and the ongoing global demographic and epidemiologic changes denote a growing cancer burden over the next decades. It is the major cause of death in economically developed countries and the second one in developing countries (Ferlay et al., 2010)

Gastric cancer (GC) is the fifth most common malignancy in the world, with an estimated 952 000 new cases to have occurred in 2012 (6.8% of total cancer incidence), behind cancers of the lung, breast, colorectal and prostate, and it is the third leading cause of cancer death in both sexes worldwide, with 723 000 deaths in 2012 (8.8% of total cancer mortality) (Ferlay et al., 2015). Generally, age-standardized incidence rates are about twice as high in men than in women and the risk is related with increased age, occurring commonly between 55 and 80 years of age and it is rare in individuals under 30 years (Piazuelo and Correa, 2013). Over 70% of cases arise in developing countries and half the world total occurs in Eastern Asia (mainly in China). In Portugal, GC ranks fifth in incidence and third in mortality (Ferlay et al., 2015). Within the country, the incidence and mortality vary between north and south regions, with both measures being higher in the north (Ferronha et al., 2012).

The development of GC is a multifactorial event that encompasses many etiologic factors and it is the result of a defined histological evolution of stomach pre-malignant lesions (Correa, 1992). This malignant neoplasia is divided into distinct subtypes based on underlying risk factors (sporadic *vs* inherited) and also on the presence of molecular and histological phenotypes. About 95% of gastric tumours are adenocarcinomas and the most commonly used histological classification for gastric adenocarcinomas is based on Laurén's criteria. The Laurén classification system divides gastric cancer into three histologic subtypes: intestinal, diffuse and indeterminate types (Lauren, 1965). Regarding their incidence, the intestinal type is the most common, followed by the diffuse and then indeterminate type (Berlth et al., 2014). Intestinal-type adenocarcinoma is more often diagnosed in males and older age groups, it progresses through a series of well-defined histological steps, which is initiated by the transition from normal mucosa to chronic superficial gastritis, then is followed by atrophic gastritis and intestinal metaplasia, ultimately leading to dysplasia and adenocarcinoma (known as Correa's cascade) (Correa, 1992). Diffuse-type carcinoma is more common in female and young individuals, it consists of poorly cohesive cells which exhibit deep infiltration of the stomach wall, with little or no gland formation (Lauren, 1965, Dicken et al., 2005)

A set of risk factors associated with the development of gastric cancer has already been described and they are based on epidemiological evidences, being possible to divide

them into two main categories: environmental risk factors and genetic alterations. Among the environmental factors, obesity (Li et al., 2012), smoking habits, heavy alcohol consumption, high salt and low intake of vegetables and fruits are important external factors for the occurrence of gastric cancer (Massarrat and Stolte, 2014). Furthermore, as well as other human cancers, gastric carcinogenesis can also be deeply influenced by genetic and epigenetic alterations (Resende et al., 2010, Shi et al., 2014). Although the development of GC implies a multifactorial event, the pathogenesis of intestinal-type GC is considered to begin from a single infectious agent, *Helicobacter pylori* (*H. pylori*) (Lu and Li, 2014).

H. pylori is a gram-negative microaerophilic bacterium that has the capacity to survive and chronically infect gastric epithelial cell surfaces and the overlying mucus protective layer (Wroblewski et al., 2010). It has been proposed as the main causative agent of chronic gastritis and ulcers and it is also associated with the development of gastric adenocarcinoma and mucosa-associated lymphoid tissue (MALT) lymphoma (Bhandari and Crowe, 2012). Data from clinical trials have demonstrated that *H. pylori* eradication therapy decreases the development of precancerous lesions and GC (Kato and Asaka, 2012). This provides further clues of the importance of this organism in early stages of gastric carcinogenesis (Mera et al., 2005). Thus, it is classified as a Group 1 carcinogen by the World Health Organization (WHO) and International Agency for Research on Cancer (IARC) (IARC, 1994). Although chronic *H. pylori* infection is the strongest known factor for the development of gastric carcinoma, most of the infected individuals stay asymptomatic over the course of precancerous lesions cascade. Between infected individuals, about 10% display peptic ulcer disease, 1-3% progress to gastric adenocarcinoma and 0.1% develop MALT lymphoma (Wang et al., 2014). The relevance of *H. pylori* infection on gastric malignancies may rely on the anatomic location. Cancers of the proximal stomach (cardia and gastroesophageal junction) have distinct epidemiological and pathophysiological features and are not frequently found in high *H. pylori* endemic areas, unlike the non-cardia gastric cancer, which has the infection as a strong risk factor (Kamangar et al., 2006). Considering the distinct morphology and functions of upper and lower stomach, *H. pylori* colonizes the antral region first (antral gastritis) and then, the inflammation process could spread upwards to corpus region with advancing age under certain conditions (corpus-predominant gastritis). The gastritis confined to the antrum can occur without *H. pylori* infection, while the progress of gastritis to the corpus is related with *H. pylori* infection in 80% of the patients (Haj-Sheykholeslami et al., 2008). Thus, corpus-predominant gastritis prompts individuals into gastric cancer, which may depend in part of reduced acid secretion (slowly disappearance of parietal cells). The atrophy of corpus-associated mucosa due to the advance of inflammation causes a change of mucosa to metaplastic type (intestinal metaplasia). On the other hand, the antrum gastritis results in increased acid production

and duodenal ulcer or pre-pyloric ulcer disease can be developed, which is associated with a decreased risk of gastric cancer (Atherton, 2006, Massarrat and Stolte, 2014).

The intestinal-type adenocarcinoma is strongly associated with environmental factors and *H. pylori*, while the diffuse-type is more often related to genetic abnormalities (Hu et al., 2012)**.** It was observed a much higher prevalence of infection in patients with intestinal-type (89.2%) when compared with patients suffering from diffuse-type (31.8%) gastric cancer (Pandey et al., 2010). When gastric cancer is early discovered, still confined to mucosa and/or submucosa and regardless of lymph node metastases, the 5-year survival rate is between 85 and 100%, whereas in advanced stage it is only 5-20% (Piazuelo and Correa, 2013). The great majority of gastric cancers occur sporadically, being intrinsically connected with a set of risk factors in which *H. pylori* has a leading role for the promotion of histological and molecular features that portray premalignant lesions. About 10% of gastric carcinomas exhibit familial clustering, but only 1-3% of gastric carcinomas emerge from inherited gastric cancer predisposition syndromes, such as hereditary diffuse gastric cancer (HDGC), among other ones(Hu et al., 2012). The lifetime risk of development GC in these syndromes is usually low, although the percentage varies substantially between populations studied (Pinheiro et al., 2014).

A growing body of evidences quotes pivotal roles for glycans on distinct pathophysiological events during cancer progression (Pinho and Reis, 2015). In the process of gastric carcinogenesis, glycans have been shown to have major impact in modulating the malignant behaviour of cancer cells associated with their cell-cell and cell-matrix interactions, migration, invasion and metastasis. Moreover, *H. pylori* colonization and infection of gastric mucosa is promoted by bacterial attachment to the gastric mucus layer and epithelial cells that present a distinctive glycophenotype (Magalhaes and Reis, 2010). Several cancer-associated features are mediated by glycosylated molecules, some of which will be further discussed in detail, with particular emphasis to their unique structural composition and associated biological functions.

Glycans and cancer

Glycans are individual or covalent sets of sugars (oligosaccharides or polysaccharides) found in free form or covalently linked to proteins or lipids (glycoconjugates) (Bertozzi CR and D, 2009). Glycans constitute the cell glycocalyx and can also be secreted and make part of the surrounding extracellular matrix (ECM) (Fuster and Esko, 2005). It is estimated that more than half of all human proteins undergo glycosylation. The occurrence of aberrant glycosylation has been strongly implicated in many different diseases, with particular worth in cancer area (Christiansen et al., 2014). Although the glycan signature cannot be reduced to simple biomolecular "fit" models owing to its complex structural information, the glycoconjugates can confer positive selective properties on cell populations (Apweiler et al., 1999). In tumour microenvironment, alterations in the glycosylation of proteins and lipids can propel neoplastic cells to begin cancer-related actions due to changes associated with their biological function (Fig.1.1) (Stowell et al., 2015).

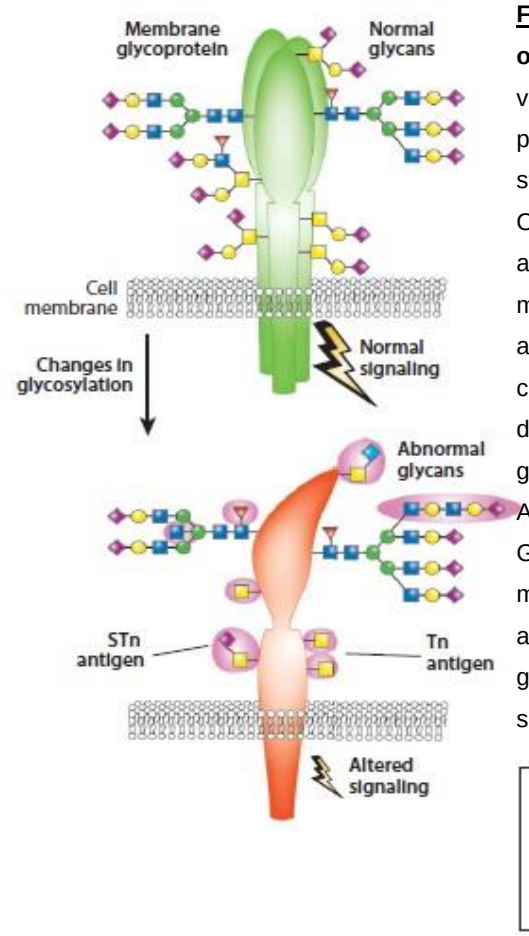

Figure 1.1: Glycosylation changes have direct influence on multiple types of glycans. These changes induce a variety of cellular responses, namely through altered signaling pathways. The most commonly glycosylation pathways studied are those which give rise to N- and O-glycans. Altered O-glycans frequently present truncated antigens (STn and Tn antigens) or sialylation, a common terminal glycan modification, being observed in both N- and O-glycans. Such alterations can become enriched on the cell surface following changes in glycosylation. There are eleven nucleotide sugar donors and multiple protein and lipid acceptor motifs for glycosyltransferases.

Abbreviations: Glc, glucose; GlcNAc, *N*-acetylglucosamine; Gal, galactose; GalNAc, *N*-acetylgalactosamine; Man, mannose; Fuc, fucose; Xyl, xylose; Neu5Ac, 5-*N*-acetylneuraminic acid (sialic acid); IdoA, iduronic acid; GlcA, glucuronic acid; Neu5Gc, 5-*N*-glycolylneuraminic acid; STn, sialyl Tn (image adapted from (Stowell et al., 2015)).

It has been notorious the importance of altered glycosylation in cancer biomarker field, with glyco biomarkers being used for cancer detection and prognosis. Several serological assays in clinical use are based on detection of glycoconjugates present in the serum of cancer patients (Reis et al., 2010).

Glycosylation is not a template based process such as DNA, RNA, or protein synthesis but is largely dependent on the balance attained by the expression and activity levels of several enzymes required for the glycosylation process, such as glycosyltransferases and glycosidases, whose major location are in endoplasmic reticulum (ER) – Golgi pathway (Caramelo and Parodi, 2007). Glycosyltransferases synthesize glycan chains, while glycosidases hydrolyse specific glycan linkages. Both types of enzymes collaborate to set up the structural glycan repertoire (Ohtsubo and Marth, 2006).There are several main families of glycoconjugates which present the sugar residues attached to core proteins or lipids in a unique and well characterized manner. The formation of the sugar-amino acid bond is a defining event which determines the nature of the carbohydrate units that will be generated by the cellular enzymatic machinery and consequently, it will define the protein biological activity (Spiro, 2002). The glycans synthetized in humans are mainly attached to the core protein in either two ways: (1) a N-acetylglucosamine (GlcNAc) residue is added to the amide group of asparagine (Asn) residue within a consensus peptide sequence of Asn-X-Ser/Thr (where X can be any amino acid except proline), featuring the *N-linked* oligosaccharides of many glycoproteins and it is the most widely distributed carbohydrate-peptide bond (Montreuil, 1980, Tuccillo et al., 2014); (2) a N-acetylgalactosamine (GalNAc) is added to the hydroxyl group of serine (Ser) or threonine (Thr) residues, giving rise to *O-linked* oligosaccharides that predominate mostly on secreted and membrane bound mucins (in tandem repeat structures, such as proline-threonine-serine domains) (Tuccillo et al., 2014). Mucins are highly glycosylated proteins present in epithelial layers of our body as protective barriers. The glycosylation pattern of mucins provides a useful tool for distinguish between healthy and diseased individuals. The healthy gastric mucosa displays MUC1, MUC5AC and MUC6 mucins. MUC1 is a membrane-associated mucin expressed in foveolar cells, while MUC5AC is secreted and limited to the foveolar epithelium and is a major component of the surface mucous gel layer. MUC6 is also secreted but is limited to deeper gastric glands (Reis et al., 1999). Although tissue-specific, mucins can be overexpressed in different locations regarding their origin. For example, MUC2 is expressed by normal intestinal mucosa, but can be aberrantly expressed in intestinal metaplasia (Reis et al., 1999, Reis et al., 2010). Glycan chains on mucins often present truncated glycans (T antigens) or terminal specific histo-blood group antigens (Lewis antigens), that can be exploited by microorganisms (including *H. pylori*) to colonize mucosal surfaces (Magalhaes and Reis, 2010, Magalhaes et al., 2015).

A particular set of heavily glycosylated proteins, called proteoglycans, are extensively produced by mammalian cells and due to their complexity and diversity, they can assume great importance in cell biology regulation.

Proteoglycans: receptors in cancer progression

Proteoglycans have been studied over the past four decades regarding their complexity, diversity and functions with a widely association in control of cell growth and survival, induction of apoptosis, adhesion and invasion (Esko et al., 2009). Proteoglycans consist of a core protein modified with linear, sulfated and negatively charged polysaccharide chains termed glycosaminoglycans (GAGs). GAGs are covalently attached to serine residues through a tetrasaccharide bond: xylose-galactose-galactose-glucuronic acid (Xyl-Gal-Gal-GlcA) (Edwards, 2012), located in sequence motifs of short serine-glycine repeats flanked by hydrophobic and acidic domains (Gallagher, 2001). GAGs chains are composed of repeating disaccharide units containing acetylated amino sugar moieties (GlcNAc and GalNAc) and mostly uronic acid (D-glucuronic acid – GlcA, or L-iduronic acid - IdoA) (Gandhi and Mancera, 2008). GAGs can be divided into two classes according to their sulfated status: (1) sulfated GAGs such as heparan sulfate (HS), chondroitin sulfate (CS), dermatan sulfate (DS), heparin and keratan sulfate (KS) and (2) non-sulfated GAGs such as Hyaluronan (HA) (Couchman and Pataki, 2012). Proteoglycans are expressed by almost all mammalian cells and can be inserted into the plasma membrane, stored in secretory vesicles or secreted into the ECM. The vast diversity of proteoglycans is due to the result of various combinations of protein cores substituted with one or more GAG chains of different subtypes that can be definitely or temporarily attached (the so-called “Part-time” proteoglycans). The stoichiometry of GAG chains is an additional cause of variability. Taking this into consideration, a given proteoglycan expressed by distinct cell types usually displays differences in GAG chains number, length and pattern of charge, acetylating and sulfating domains (Esko et al., 2009). There are several ways to classify the proteoglycans by groups based on their location and binding, predominant GAG chains or according to the properties of their core proteins (Schaefer and Schaefer, 2010, Edwards, 2012). According to cellular localization, proteoglycans can be divided in three groups: (1) proteoglycans present in ECM, such as small leucine rich proteoglycans (SLRPs; ex: decorin, biglycan and lumican), hyalectans (ex: aggrecan, versican, neurocan and brevican) which associate with hyaluronan in ECM and the basement membrane proteoglycans (ex: perlecan, collagen XVIII and agrin); (2) plasma membrane-associated proteoglycans, such as the syndecans and the glycosylphosphatidylinositol-anchored glypicans and (3) the intracellular proteoglycan serglycin which is present in secretory vesicles of endothelial and hematopoietic cells (Theocharis et al., 2010).

A solid knowledge has been presented over the past years regarding the fundamental roles of heparan sulfate proteoglycans in important biological functions. Next, it will be given emphasis to this particular group of proteoglycans whose localization is scattered over the cells and ECM and that are involved in effects at cellular, tissue and organism level.

Heparan sulfate proteoglycans

The cell surface heparan sulfate proteoglycans (HSPGs) are involved in monitoring ligand-receptor interactions and extracellular matrix HSPGs are considered important modulators of intercellular molecular traffic. Some HSPGs also contain CS/DS chains that diverge from HS in its sugar components (GalNAc and GlcA/IdoA) and modification patterns (Rapraeger et al., 1985, Couchman, 2010). One example of such proteoglycan is the syndecan 1, bearing both HS and CS chains on its extracellular domain (Szatmari and Dobra, 2013). There are evidences suggesting that HS and CS biosynthesis are in close association, possibly due to the sharing of similar linkage sites, where the absence of one allows the replacement by the other (Kreuger and Kjellen, 2012). HSPGs bind to an extensive variety of ligands, frequently via HS chains. Indeed, a highly sulfated form of HS called heparin, that is exclusively synthetized by connective-tissue type mast cells as serglycin proteoglycan (Schaefer and Schaefer, 2010), is usually used as an “affinity” matrix for the purification of a wide range of biomolecules, having given rise to the heparin chromatography technique (Xiong et al., 2008). GAG-binding proteins have multiple domains that juxtapose positively charged amino acids (lysine and arginine) that can interact with the negatively charged sulfates and carboxylates of the GAG chains. These sequences are present in ligands such as cytokines and growth factors. Sugar residues located within the chain or near the terminus are used for the binding of proteins (Esko et al., 2009). Even though some ligands can bind directly to HSPG core proteins, the basis connection occurs through the HS chains.

The HS chains can have variable length and can diverge regarding the degree and pattern of sulfation. Therefore, the 32 potential exclusive disaccharide units and their combination into structural motifs potentiate this class of compounds to reach high relevance in biology field. This suggest a great grade of complexity and non-template-driven biosynthesis regarding HS chains, where their functions appear from the disposal and density of certain domain patterns (i.e. local disposal of several sequence clusters), instead of protein function that can be assessed through its unique folded structure (Nugent et al., 2013). In theory, the fine structure of HS chains can bind to an infinite number of protein-binding epitopes, although it is dependent of substrate specificities and enzyme-related expression that significantly restrict the number of HS epitopes expressed (Rudd and Yates,

2012). The core protein that shelter the HS chains may be a restrictive factor on HS biosynthesis related to types and amounts of HS presented at the cell surface (i.e. attached to syndecans and glypicans) and/or in the ECM (i.e. attached to agrin, perlecan and collagen XVIII). It has also been shown that other GAGs-unrelated domains can have regulatory functions (Chen and Lander, 2001). Regarding the tetrasaccharide Xyl-Gal-Gal-GlcA linkage between the extended HS chain and the core protein, it may be altered by sulfation of the two Gal units and phosphorylation of the Xyl unit. These alterations can disturb downstream enzymatic polymerization activities (Kreuger and Kjellen, 2012).

Heparan sulfate chains are characterized by long linear chains of repeating disaccharide units (40-300 sugar residues, ~20-150 nm), alternating N-substituted glucosamine and hexuronic acid residues dependent on selective modifications comprising sulfation of the N-position as well as the C-6 and C-3 O-positions of the glucosamine residue and the C-2 O-position of the iduronic acid (Fig. 1.2) (Sarrazin et al., 2011). The specific chain structure is the outcome of 18 enzymes, anchored to the Golgi membrane, as well as two postsynthetic 6-O-endosulfatases and extracellular heparanase, the latter being crucial in trimming the less-sulfated regions along the HS chains and giving rise to smaller (10-20 sugar residues) and potentially bioactive HS fragments (Manon-Jensen et al., 2010, Nugent et al., 2013). *In vitro* results appoint to sulfation content importance of the growing HS backbone for the polymerization and chain elongation (Lidholt and Lindahl, 1992).

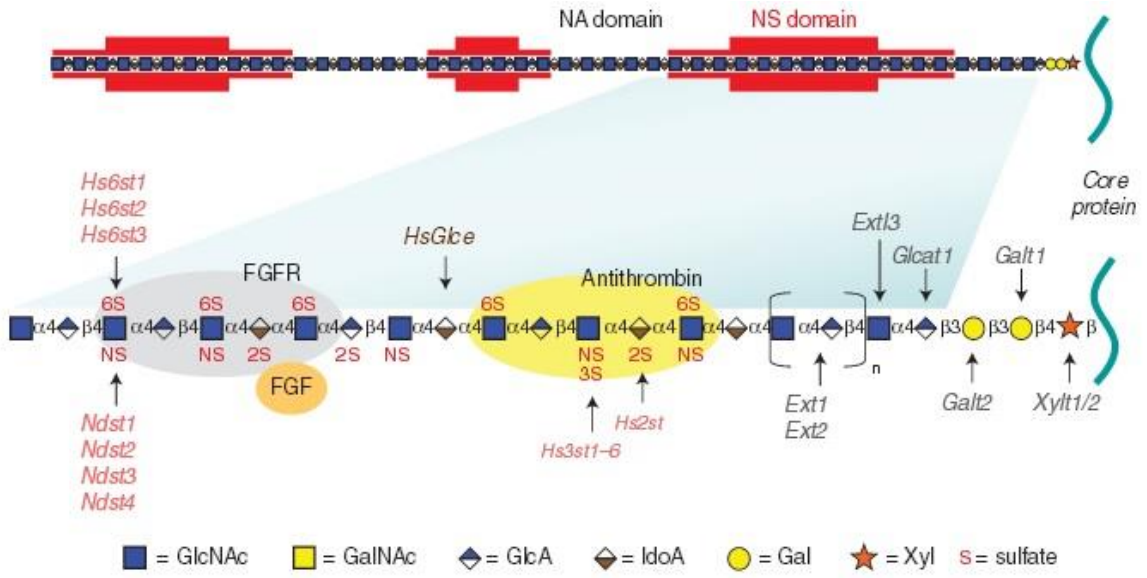

Figure 1.2: Schematic representation of heparan sulfate synthesis and its modifications. HS chain synthesis starts by the attachment of linkage tetrasaccharide (GlcA-Gal-Gal-Xyl) to serine residues of the core protein. Next, the first GlcNAc unit is added by Exostosin-like 3 (EXTL3), following addition of GlcNAc and GlcA units to the nascent chain by the EXT1/EXT2 polymerase complex. The disaccharide residues undergo a series of modification reactions, beginning with N-deacetylation/N-sulfation by one or more N-deacetylase/N-sulfotransferases (NDSTs), followed by epimerization of GlcA to IdoA (by C5 epimerase - HsGlce) and 2-O-sulfation (by 2-O-sulfotransferase – Hs2st) and finally 6-O-sulfation (by Hs6st1-3) and 3-O-sulfation (by Hs3st1-6) at glucosamine units. The modifications happen in clusters of variable length (NS or NA domains) (Sarrazin et al., 2011).

The ultimate HS products exhibit a highly variable domain-type arrangement in which N-sulfated regions (NS domains, rich in N-sulfated glucosamine units) are separated by non-modified N-acetylated regions (NA domain). Occasionally, intermediate regions alternating N-sulfated and N-acetylated glucosamine units can surround the NS domain (NA/NS domains). Both of these specific regions may have different lengths, although the length of the NS domain is strongly correlated with the concentration of the sulfate donor 3´-phosphoadenosine-5´-phosphosulfate (PAPS) (Carlsson et al., 2008). Hence, for the biosynthesis of HS chains is required not only UDP-sugars, but also the sulfate donor PAPS, being both of these precursors produced in the cytosol and transported into the Golgi compartment (Caffaro et al., 2006).

The large amount of ligands for few HSPGs implies that the main roles of HS are to concentrate ligands or manage their content within tissues. Protein ligands may connect with single NS domains rich in O-sulfate groups or with two NS domains separated by N-acetylated residues (Kreuger and Kjellen, 2012). It has been well characterized the interaction concerning heparin (a processed, vastly sulfated form of HS) and HS with fibroblast growth factors (FGFs) and their receptors (FGFRs) and between heparin and antithrombin (illustrated in Fig.1.2). Features such as size, fine structure and ligand affinity

of the HS chains on single HSPG species seem to vary between cell types, which can enable cells to react differently to HS-binding effectors present in the microenvironment (Kato et al., 1994).

HSPGs are considered as “full-time” if their role is limited to HS action on cell signalling, or “part-time” if they present further structural variability which confers them different roles in numerous signalling pathways. One sub-group of “full-time” HSPGs are the four transmembrane syndecans which cellular localization prompts them to have mediator roles in cell proliferation, differentiation, adhesion and migration through interaction with a wide range of ligands such as structural ECM molecules, cytokines, chemokines, growth factors and enzymes. Such interactions are dependent of phosphorylation, induced membrane clustering and shedding of the syndecan extracellular domain (Tkachenko et al., 2005). It has been demonstrated that abnormal syndecan regulation has significant impact in several pathologies, including inflammation, wound healing and cancer.

Syndecans: versatile transmembrane receptors

Syndecans (SDCs) are an evolutionarily conserved family of type I transmembrane heparan sulfate proteoglycans consisting in four different members and all cells express at least one type of SDC. Each SDC family member has a characteristic temporal and spatial pattern of expression. SDC1 is common in epithelial and plasma cells; SDC2 is present in endothelial cells, fibroblasts, smooth muscle cells and neurons; SDC3 is expressed in neural tissue and the developing musculoskeletal system, whereas SDC4 is ubiquitously distributed (Barbouri et al., 2014). Structurally, the SDCs core proteins range from 20 to 40 KDa and are divided into three distinct and characterized domains: an N-terminal extracellular domain (ED) that contains consensus sequences for bearing 3-5 HS chains, although additional CS/DS chains can also be linked; a transmembrane domain (TM) composed of 25 hydrophobic amino acid residues responsible for homodimer/oligomer formation between SDC core proteins (due to a conserved GXXXG motif in this domain) which is essential for signal transduction between ECM to the cytosol, and a short C-terminal cytoplasmic domain (CD) consisting of a membrane-proximal conserved C1 region and a C-terminal C2 region, both of them flanking a variable region (V) that is unique to each SDC (Fig. 1.3) (Lambaerts et al., 2009, Choi et al., 2011).

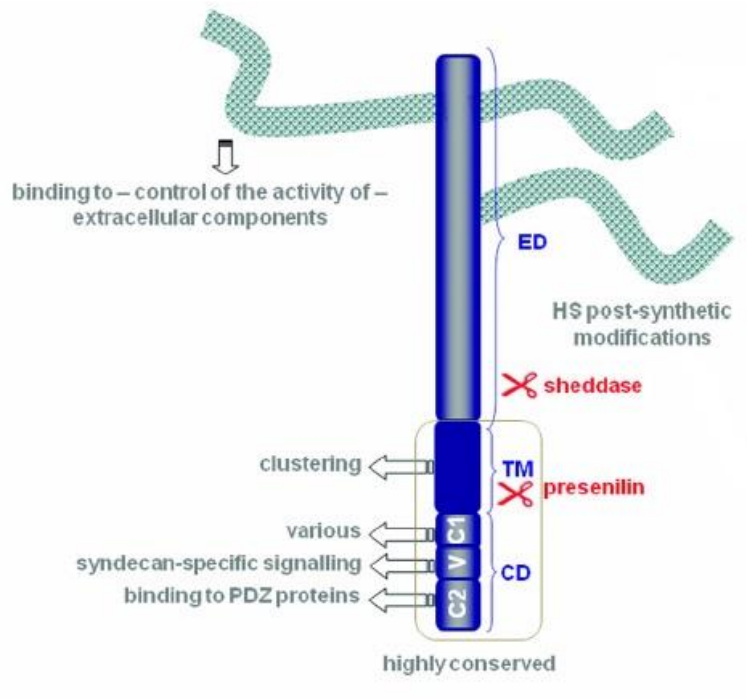

Figure 1.3: Syndecan structure. The core protein is divided into 3 domains: extracellular (ED), transmembrane (TM) and cytoplasmic domain (CD). The specific functions of each domain are dependent on the type of ligands. The syndecan ED can be cleaved by sheddases at membrane-proximal sites which results in separation from the remaining TM and CD. Both TM and CD are then processed by presenilin, being released to the cytosol (image adapted from (Lambaerts et al., 2009)).

Both TM and CD are highly conserved among SDC family members and across species, in contrast with the ED that is very divergent in size and amino acid sequences (sharing only attachment sites for GAG chains and proteolytic cleavage sites), indicating that distinct and unique functions may depend of this domain (Beauvais and Rapraeger, 2004). Growing evidences suggest that SDC core proteins *per se* are involved in selective ligand binding, giving rise to further SDC-dependent interactions. The ED of SDCs can be cleaved at juxtamembrane sites by particular sets of enzymes referred to as sheddases, which convert membrane-bound SDCs into soluble effectors or antagonists. The transmembrane receptor portion that remains after cleavage ends up losing its ability to bind external ligands and it is processed through intramembrane cleavage by the presenilin/γ-secretase complex (Manon-Jensen et al., 2010). These soluble SDC ectodomains compete with intact membrane-associated SDCs for the broad set of ECM ligands and contribute for their importance in tumourigenesis (Choi et al., 2011).

The cytoplasmic domains of SDCs are of extremely importance for downstream intracellular signalling that defines morphological and biological changes in cell behaviour. These domains are small in length, some 40 amino acids or less and they have no intrinsic enzymatic activity (Couchman et al., 2015). The 3 sub-regions comprising the CD have

particular cytoplasmic-associated ligand interactions which translate multiple SDC-dependent actions throughout the cell. The C1 region contributes to linkage to actin-associated cytoskeleton through ezrin-radixin-moesin (ERM) proteins, cortactin and tubulin interactions. It also binds to dynamin, which is suggested to be mechanistically linked to endosome formation (Lambaerts et al., 2009). The C2 region (located at the C-terminal site) consists in the amino acid sequence EFYA that is common to all SDCs and it binds to PDZ domains in several proteins, such as syntenin, synectin, synbindin and calcium/calmodulin-dependent serine/threonine kinase (CASK), thus modulating cell polarization, recycling and regulation of trafficking (Multhaupt et al., 2009). The V region enables SDC-specific signalling for each SDC member which turns the identification of interactions and functions a defiant process regarding all SDC family (Oh et al., 1998). In particular, the V region of SDC4 binds to phosphatidylinositol -4,5- bisphosphate ($PI4,5P_2$) and protein kinase Cα (PKCα) and these interactions are crucial for actin microfilament bundle contraction (stress fibers) and focal adhesion assembly (Okina et al., 2009).

Syndecan-4 and β1 integrin interactions

Syndecan-4 expression is low comparatively to the other SDCs, although its distribution throughout the human body is ubiquitous. It has been assigned pivotal and diverse roles in wound healing, arterial development, immunosuppression and cancer biology (Elfenbein and Simons, 2013). Abnormal expression of SDC4 is described in breast cancer, hepatocellular carcinoma, melanoma and malignant mesothelioma. The SDC4-dependent signalling is more significant for morphology and behaviour of cells rather than having a transcriptional impact on specific genes (Couchman et al., 2015). This membrane proteoglycan as well as its shed ectodomain have established functions regarding the adhesion to components of the ECM, such as fibronectin through its HepII heparin-binding domain. This generates cell cytoskeletal modifications and activation of signalling pathways that drive to the formation of focal adhesions, localized membrane regions with typically increased tensile strength, and stress fibers (enrichment of cytoskeletal proteins, including vinculin, paxillin and actin) (Woods and Couchman, 2001). SDC4 is the only member of the SDC family that is enriched in focal adhesions. Moreover, transfections experiments with a truncated form of SDC4 that lacks the cytoplasmic V region decreased focal adhesion formation and consequently reduced cell spreading (Longley et al., 1999). Focal adhesions are key regions where cells apply mechanical forces on the matrix which affects wound healing and tumour-stroma interactions.

SDC4 has a central role by mediating focal adhesion formation through engagement of integrins, another family of transmembrane glycoproteins. The integrin family is composed by 24 α,β-heterodimeric members, being encoded 18-α and 8-β different

subunits by the human genome. The α-subunit determines integrin ligand specificity, while the β-subunit is responsible for connection to cell cytoskeleton and contributes to multiple signalling pathways (Barczyk et al., 2010).The integrin-ECM linkage is accomplished by a specific arginine-glycine-aspartate (Arg-Gly-Asp) sequence (RGD motif), which is present in fibronectin, vitronectin and tenascin (Humphries et al., 2006). Another significant feature for substrate binding and normal transport to the cell surface is the N-glycan content of integrins. Indeed, α5β1 integrin, which is one of the best-characterized integrins, requires N-glycans for αβ heterodimer formation and integrin-matrix interactions (Pinho et al., 2013). The bi-directional signalling ability (outside-in and inside-out) and the conformational changes of integrins are important for focal adhesion assembly and genetic analysis of mutant integrins have shown roles in tissue structure and cell migration (Bouvard et al., 2001).

The interplay between SDC4 and α5β1 integrin regarding focal adhesion formation is well established and this is a PKCα-dependent process that regulates the endocytosis and recycling of α5β1 integrin which allows cell migration and formation of new focal complexes (Morgan et al., 2007). It is suggested that SDC4 performs the initial contacts with the ECM, through a potential reach of 500 nm of HS chains that is ideal for capture distant ligands, and then moved laterally due to actin polymerisation to permit integrin binding, which in contrast , has a maximum reach of 17 nm (Roper et al., 2012). Indeed, SDC4 is required for a complete adhesion-dependent signalling response and acts as the early fibronectin sensor, while α5β1 integrin just provides the mechanical connection (Lin et al., 2005). To accomplish a more efficient interplay between SDC4 and α5β1 integrin, a family of Rho GTPases (Rac, Rho and Cdc42) can be alternatively activated by the synergistic SDC4-α5β1integrin signalling pathways. These small GTPases act as molecular switches to translate extracellular signals into intracellular changes that directly influence both receptors association and actin cytoskeleton reorganization (Fig. 1.4) (Brooks et al., 2012).

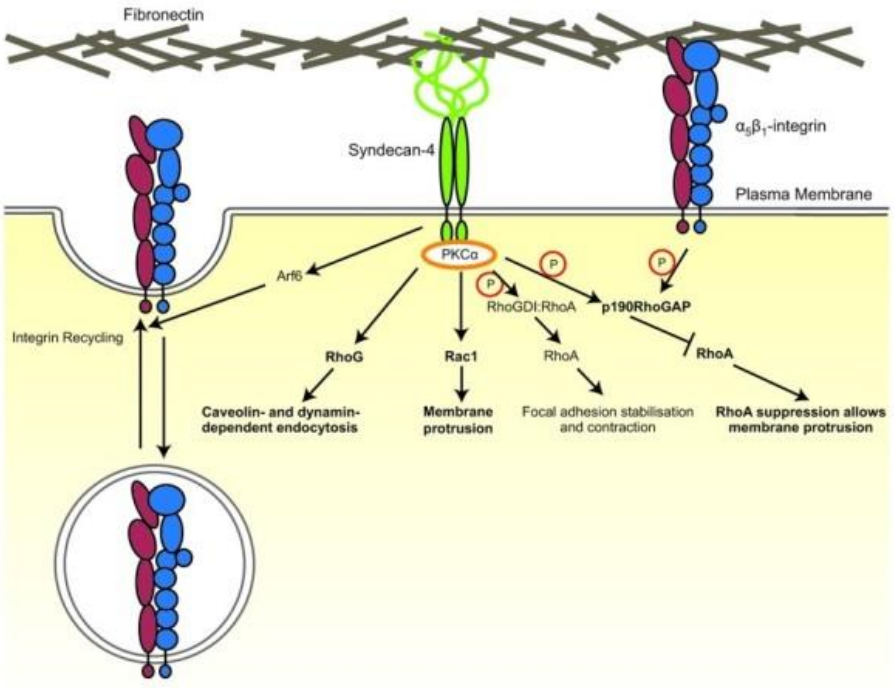

Figure 1.4: Regulation of multiple GTPases by syndecan-4 and α5β1 integrin. The activation of RhoG, which triggers the endocytosis of α5β1 integrin, and Rac1, which drives membrane protrusion and the formation of nascent focal complexes are the early signals. The activation of Rac1 leads to simultaneous RhoA suppression, due to its induced contractile signal. All these signals stimulate cell migration after SDC4 binding to fibronectin. The late signals include activation of Arf6, which helps the integrin recycling to the membrane, and reactivation of RhoA that drives focal adhesion maturation and actin filament bundling. SDC4 and α5β1 integrin affect the activity and localization of p190RhoGAP, which modulates the activation status of RhoA, thus providing a link between integrin and SDC4 signalling (Brooks et al., 2012)

The ability of cancer cells to invade into surrounding tissues relies on cycles of membrane protrusion, attachment and cytoskeleton contraction, which promotes forward movement. The formation of finger-like structures, known as filopodia, and sheet-like structures, known as lamellipodia, generate just beneath the plasma membrane the locomotive forces in migrating cells. Both structures are derived from polarized assembly of the actin cytoskeleton that helps the cell to move through the ECM. It also allows the cells to break away from the collective invasive front and change to individual migration/invasion programs (Machesky, 2008). Each Rho GTPase member plays well-characterized roles in the regulation of actin cytoskeleton organization and dynamics. This organization is typically characterized by two distinct phases: (1) early adhesion associated with pathways that stimulate membrane protrusions and (2) the maturation of such adhesions through creation of tension (DeMali et al., 2003). SDC4 and α5β1 integrin co-localize in early adhesion sites and ligand binding by both receptors is necessary for downstream signaling (Bass et al., 2007). Therefore, during cell movement, localized signaling happens by alternative activation cycles of Rac1, which promotes lamellipodia formation, and/or Cdc42, which

promotes filopodia extension, at the leading edges of the cell. Subsequently, RhoA activation drives maturation of focal adhesions and contraction of the cell body (Matsuoka and Yashiro, 2014). SDC4 and α5β1 integrin act cooperatively regarding cell spreading and maturation of adhesions as well as directional migration.

Although a growing body of evidences supports the role of SDC4 in the modulation of cancer cell behaviour, namely in the activation of aggressive cancer features as cell motility, its functional implications in GC progression remain unknown.

2. Aims of the study

The general aim of this work was to determine the molecular role of SDC4 in modulating gastric cancer cell behaviour and therefore, gastric cancer biology.

To achieve this general aim, we have focused on the following specific objectives:

- → To efficiently induce a transient silencing of SDC4 expression levels in a human gastric cell line;
- → To evaluate the influence of SDC4 transient knockdown over β1 integrin expression levels and cellular localization;
- → To examine cell morphology alterations upon SDC4 transient knockdown by the observation of specific cytoskeletal proteins;
- → To assess the contribution of SDC4 transient knockdown in gastric cell migration and invasion;
- → To characterize SDC4 expression in human gastric carcinomas and corresponding metastasis.

3. Material and methods

Cell culture

Human gastric cancer cell line AGS (Barranco et al., 1983) (derived from poorly differentiated gastric adenocarcinoma) was obtained from American Type Culture Collection (ATCC, CRL-1739™). AGS cells were cultured in RPMI-1640 (1X)+GlutaMAXTM-I medium (Gibco®, NY, USA) supplemented with 10% (v/v) fetal bovine serum (FBS, gold heat inactivated, PAA, Piscataway, NJ, USA) and 1% (v/v) penicillin-streptomycin (PenStrep, 10,000 units/mL of penicillin and 10,000 µg/mL of streptomycin., Gibco®, NY, USA) and incubated at 37ºC in humidified air with 5% CO2. Cells were maintained at low passages for siRNA transfections and functional assays.

siRNA transfection for SDC4 transient knockdown

Small interfering RNAs (siRNAs) were designed against the SDC4 mRNA sequences. Three single 27mer duplex sequences: $siRNA_A$ (5'- AGAAACUAGAGGAG-AAUGAG GUUAT-3'), $siRNA_B$ (5'- CUAUUCUAGAGAACUAAACUGGCTT-3') and $siRNA_C$ (5'GGAUUGGAUCACUUCUUAAACUUCC-3') (SR304301, OriGene Technologies, Rockville, MD, USA) were tested separately (siRNA A, siRNA B and siRNA C) and combined (siRNA ABC) for SDC4 efficient knockdown. The siRNA transfection protocol was executed according to manufacturer's instructions (Invitrogen™, CA, USA)**.** AGS cells were plated in 6-well plates ($1x10^5$ cells/well) 48h prior to transfection in 2mL of RPMI-1640 medium supplemented with 10% FBS and 1% PenStrep. The day before transfection medium was exchanged for RPMI-1640 medium supplemented with 10% FBS. The siRNA transfection assay was performed with 70-80% confluent AGS cells. The transfection protocol started with growth medium removal, the cells were washed twice in phosphate-buffered saline (PBS) and 1 mL and 750µL of Opti-MEM® reduced serum medium (Gibco®, NY, USA) was added to control cells and cells to be transfected, respectively. The 6-well plates were placed at 37ºC in humidified air with 5% CO2 during preparation of siRNAs dilutions. Single siRNA duplexes (20µM each) and the combined $SiRNA_{ABC}$ were diluted to a final concentration of 50nM and 100nM per well. First, the universal scrambled negative control siRNA, single and combined siRNAs were diluted in Opti-MEM® in one tube and in the other tube lipofectamine® 2000 reagent (1mg/mL, Invitrogen™, CA, USA) was diluted in Opti-MEM® (5µL per well) and both tubes were left at room temperature for 15 min. Then, lipofectamine® 2000 solution was added to scrambled negative control, single and combined siRNAs tubes, mixed gently and incubated for 15 min at room temperature to allow complexes to form. Finally, 250µl of each siRNA-lipofectamine® 2000 complexes were added per well (1mL of final volume per well) and the plates were incubated at 37ºC. After 6h of incubation, the transfection medium was removed, the cells were washed once

with PBS and 2mL of RPMI-1640 medium supplemented with 10% FBS and 1% PenStrep was added per well. Different time-points were used for protein extraction (24h, 30h, 48h and 72h). For RNA extraction, cells were collected at 48h time-point. The siRNA transfection efficiency was assessed by western blot and real-time PCR analysis.

Protein extraction and quantification

Protein extraction was performed in siRNA-transfected AGS cells at several time-points as previously mentioned. The protein extraction protocol started by removal of growth medium and washing cells twice with PBS. Then, 100 µL of lysis buffer RIPA (50mM Tris-HCl pH=7.4, 150mM NaCl, 2mM EDTA, 1.0% NP-40 and 0.1% SDS) containing 1mM PMSF, 1mM Na3VO4 and protease inhibitor cocktail (Roche, Germany) was added to each well. The plates were placed on ice for 10 mints, and then the cells were scraped off the wells using cell scrapers and cell lysates were collected to tubes. The tubes were placed in ice for 10 min, vortexed every 5 min and then centrifuged at 16000g for 10 min at 4ºC. This separates the total protein (supernatant) from the cellular debris (pellet). The supernatants were transferred to new tubes for protein quantification and western blot analysis.

The quantification of the extracted protein was done using the Bio-Rad DC™ Protein Assay Kit (Bio-Rad, CA, USA) according to the manufacturer´s instructions. The assay relies on the reaction between proteins and copper in an alkaline medium and the subsequent reduction of Folin reagent, which gives rise to a blue color reaction product, whose absorbance is measured at 750nm. A series of eight dilutions of bovine serum albumin (BSA, Sigma-Aldrich®, MO,USA) were prepared as protein standard solutions (maximum BSA standard concentration was 2000µg/mL and the minimum was 50µg/mL) which allows the creation of a standard curve for relative protein quantification. Each protein sample was diluted 1:2 in water and 5µL of standard BSA solutions and diluted protein samples were added in triplicate to 96 wells plates. To each well was added 25µL of reagent A' (reagent A and reagent S mixed together previously to addition), and finally 200µL of reagent B was added to each well. After 15 min, absorbances were read at 750nm on SYNERGYMx Fluorimeter (BioTek®, VT, USA). The protein samples were stored at -20ºC for further use.

Western blot

Protein expression levels of SDC4 were evaluated by western blot (WB) using an anti-SDC4 mouse monoclonal antibody (5G9**,** sc-12766, Santa Cruz Biotechnology, TX, USA) and an anti-SDC4 rabbit polyclonal antibody (H-140, sc-15350, Santa Cruz Biotechnology, TX, USA). After protein quantification, 30 µg of protein from each sample were mixed with water and 4x loading buffer (277.8mM Tris-HCl pH=6.8, 44.4% (v/v)

glycerol, 4.4% SDS, 355mM 2-mercaptoethanol and 0.02% bromophenol blue) and denatured at 95ºC for 5 min. The electrophoretic separation of proteins was done in 12% Tris-Glycine SDS PAGE gel. Briefly, a resolving gel containing 12% (v/v) acrylamide/bis-acrylamide (37.5:1), 0.375M Tris-HCl pH=8.8, 0.05% (v/v) SDS, 0.1% (w/v) APS and 0.1% (v/v) TEMED and a stacking gel containing 4% (v/v) acrylamide/bis-acrylamide (37.5:1), 0.128M Tris-HCl pH=6.8, 0.1% (v/v) SDS, 0.1% (w/v) APS and 0.1% (v/v) TEMED were prepared. The proteins were separated in the Mini-PROTEAN® Electrophoresis system (Bio-Rad, CA, USA) in Tris/Glycine SDS running buffer at 120V for 90 min.

Proteins were then transferred to a 0.45µm Nitrocellulose Blotting Membrane (GE Healthcare, Life Sciences, OH, USA) through the Mini Trans-Blot® cell system (Bio-Rad, CA, USA) in Tris/Glycine transfer buffer at 60V for 90 min. After electroblotting, membranes were incubated in blocking solution (5% (w/v) milk in PBS-Tween 20 (0.05%) for 1h at room temperature. The membranes were then incubated with anti-SDC4 primary antibodies (5G9 and H-140) diluted in blocking solution (1:500) overnight at 4ºC. After three washing steps with PBS-T (0.05%), the membranes were incubated with horseradish peroxidase-conjugated goat anti-mouse IgG secondary antibody (sc-2005, Santa Cruz Biotechnology, TX, USA) diluted in blocking solution (1:2000) for 1h at room temperature. After three washing steps with PBS-T (0.05%), membranes were subjected to chemiluminescence detection through ECL™ and Amersham Hyperfilm™ (GE Healthcare, Life Sciences, OH, USA) exposition. To ascertain equal loading of protein, membranes were incubated with anti-actin (I-19) rabbit polyclonal antibody (sc-1616-R, Santa Cruz Biotechnology, TX, USA) diluted in blocking solution (1:4000) and the same protocol was performed for actin bands detection.

RNA extraction and quantification

Cell pellets were obtained after specific siRNA transfection time-points for subsequent RNA extraction using TRI Reagent® (T9424, Sigma-Aldrich®, MO,USA) according to manufacturer's instructions and standard protocol (Chomczynski, 1993). 500µL TRI Reagent® was added to the cell pellets and repetitive pipetting was done to form a homogenous lysate that was incubated at room temperature for 5 min. It was then added 100µL of chloroform to lysates and vortexed for 15 seconds and incubated at room temperature for 15 min. The resulting mixture was centrifuged at 12000g for 15 min at 4ºC which enabled the formation of three distinct phases: a lower pink organic phase (containing proteins), an interphase (containing DNA) and a colorless upper aqueous phase (containing RNA). The aqueous phases were transferred to new tubes and 250µL of 2-propanol was added. The tubes were inverted by hand and incubated at room temperature for 10 min. Afterwards, a new centrifugation at 12000g for 10 min at 4ºC was done which yielded RNA pellets. The supernatants were removed and the RNA pellets were washed with 500µL of 75% ethanol, vortexed briefly and centrifuged at 12000g for 5 min at 4ºC. This washing step was repeated once. Finally, the supernatants were removed, the RNA pellets were air dried for 30 min and then resuspended in a variable volume of sterile water (20-30µL), according to the pellet sizes. The RNA samples were stored at -80ºC.

RNA quantification was done using NanoDrop ND-1000® UV-Vis spectrophotometer (NanoDrop Technologies, USA). The RNA samples were placed in ice for 30 min and then RNA concentrations (ng/mL) were obtained by pipetting 1µL of RNA onto an optical measurement pedestal.

Reverse transcriptase PCR (RT-PCR)

First strand cDNA synthesis using Superscript® II Reverse Transcriptase (Invitrogen™, CA, USA) was performed starting from 2µg of RNA. The corresponding volumes of RNA, 1µL of random hexamers (Invitrogen™, CA, USA) and sterile water were added to PCR tubes (11µL of final volume) and the mixtures were heated at 65ºC for 5 min in thermal cycler 2720 (Applied Biosystems™, CA, USA) and subsequently chilled on ice. The RT-PCR Mix was prepared by addition of sterile water, 5x First-Strand Buffer, 0.1M DTT, dNTPs, RNaseOUT™ (40U/µL) and Superscript® II RT (200U/µL) (Invitrogen™, CA, USA) and then 9µL of the total mixture was added to each PCR tube containing the RNA. The PCR tubes were placed in the thermal cycler and incubated at 25ºC for 10 min, 42ºC for 50 min and 70ºC for 15 min. Finally the PCR products were stored at -20ºC.

Real-time PCR

Real-time PCR (qPCR) was based on TaqMan® Gene Expression Assays (TaqMan® MGB probes, FAM™ dye-labeled) (Applied Biosystems™, CA, USA) according to manufacturer's instructions. This method was used for quantitative detection of SDC4 and β1 integrin genes. 18S gene was used as an endogenous control to normalize the RNA total levels of each sample. Briefly, the reaction conditions consisted in a 10µL final volume containing 3.5µL of sterile water, 1µL of cDNA, 5µL of 2x TaqMan® Universal PCR Master Mix, No AmpErase® UNG (Applied Biosystems™, CA, USA) and 0.5µL of 20x TaqMan® Gene Expression Assay Mix for SDC4 (HS00161617_m1), β1 integrin (HS00559595_m1) or 18S (HS99999901_s1**).** The reactions were carried out in a 7500 Fast Real-Time PCR system (Applied Biosystems™, CA, USA) as follows: 50ºC for 2 min, 95ºC for 10 min, 40 cycles at 95ºC for 15 seconds and 60ºC for 1 min. Triplicates were performed for each sample.

Double immunofluorescence

Immunofluorescence protocol was performed with siRNA transfected AGS cells which were plated on 12 mm diameter coverslips in 6-well plates ($5x10^4$ cells/well) 72h prior to transfection in 2mL of RPMI-1640 medium supplemented with 10% FBS and 1% PenStrep. An overnight coating of coverslips with 10%FBS was previously performed at 37ºC in humidified air with 5% CO2. After 48h of transfection assay, the coverslips were fixed with 4% paraformaldehyde (PFA) and stored at -20ºC.

The coverslips were washed twice with PBS and NH_4Cl (50mM, diluted in PBS) was added for 10 min at room temperature. Then, three washes with PBS were done and cellular membrane permeabilization was performed with 0.2% Triton X-100 (Sigma-Aldrich®, MO,USA) in PBS for 5 min at room temperature. Then, two washes with PBS were performed and the cells were incubated in goat normal serum (Dako, Glostrup, Denmark) diluted in 10% BSA/PBS (1:5) for 20 min at room temperature. The serum solution was removed and coverslips were incubated with anti-SDC4 mouse primary monoclonal antibody (5G9) diluted in 5% BSA/PBS (1:40) overnight at 4ºC.

The next day, the coverslips were washed twice with PBS and incubated with goat anti-mouse IgG2a secondary antibody conjugated with Alexa Fluor® 488 (A21131, Invitrogen™, CA, USA) diluted in 5% BSA/PBS (1:250) for 1h at room temperature and protected from light. From this step, the protocol was performed with coverslips always protected from light. Two washes with PBS were done and coverslips were incubated with anti-β1 integrin primary monoclonal antibody (4B7R, ab3167, Abcam®, Cambridge, UK) diluted in 5% BSA/PBS (1:200) for 2h at room temperature. The coverslips were washed

twice with PBS and incubated with goat anti-mouse IgG1 secondary antibody conjugated with Alexa Fluor® 594 (A21125, Invitrogen™, CA, USA) diluted in 5% BSA/PBS (1:250) for 1h at room temperature. The cells were washed twice with PBS and incubated with DAPI (Sigma-Aldrich®, MO,USA) diluted in PBS (1:100) for 15 min at room temperature. Two more washes with PBS were performed and the coverslips were mounted on glass slides with Vectashield (Vector Laboratories, CA, USA). Negative controls were performed by replacing the primary antibodies with PBS. Secondary antibodies specificity was also tested by cross combination with both primary antibodies. The immunofluorescence analysis was made on fluorescence microscope (Zeiss Axio Imager.Z1) and the images were obtained by AxioVision Imaging System software.

The same protocol was adapted for fluorescence staining of tubulin and actin. The siRNA transfected AGS cells were incubated with anti-α-tubulin IgG1 mouse monoclonal antibody (T9026, Sigma-Aldrich®, MO,USA) diluted in 5% BSA/PBS (1:750) overnight at 4ºC. For fluorescence labeling of tubulin, the coverslips were incubated with goat anti-mouse IgG (H+L) secondary antibody conjugated with Alexa Fluor® 488 (A11029, Invitrogen™, CA, USA) diluted in 5% BSA/PBS (1:500) for 45 min at room temperature. After the washing steps, the coverslips were incubated with anti-actin (I-19) rabbit polyclonal antibody (sc-1616-R, Santa Cruz Biotechnology, TX, USA) diluted in 10% BSA/PBS (1:150) for 45 min at room temperature. The secondary antibody used for actin labeling was the goat anti-rabbit IgG (H+L) antibody conjugated with Alexa Fluor® 594 (A11037, Invitrogen™, CA, USA) diluted in 5% BSA/PBS (1:500) for 45 min at room temperature.

Migration assay

Cell migration was analyzed using two wells µ-Dishes^{35mm,high} with culture-inserts (Ibidi®, Munich, Germany) according to manufacturer's protocol. Migration assays were performed on AGS cells which were transfected with 50nM of scrambled negative control siRNA (siCTRL) and siRNA ABC (siSDC4) 12h before. Briefly, 5x10^4 cells in 70µL of RPMI-1640 medium with 10% FBS were applied into each well and incubated at 37ºC with 5% CO2. After proper cell attachment was achieved (24h) the insert was removed creating a 500µm cell free gap. Phase contrast images of the same gap fields were captured at 0h, 3h, 6h, 9h and 12h of incubation using the CKX41 inverted phase contrast microscope (Olympus®, Tokyo, Japan) and decrease of cell-free area was quantified through ImageJ software (NIH).

Invasion assay

Cell invasion capacity was assessed using BioCoat™ Matrigel® Invasion Chambers with 8µm PET membranes (Corning Inc., NY, USA). Invasion assays were performed using AGS cells which were transfected with 50nM of siCTRL and siSDC4 24h before. Briefly, 7x10^4 cells in 500µL of RPMI-1640 medium were seeded on the upper part of invasion chambers and incubated at 37ºC in humidified air with 5% CO2. The RPMI-1640 medium with 10% FBS was added to the lower part of chambers (750µL/well) and incubated at 37ºC with 5% CO2. After 24h of incubation, the chambers were washed with PBS and the cells that remained on the upper membrane were removed with a cotton swab. The cells were fixed with cold methanol for 10 min and the membranes were mounted on glass slides with Vectashield with DAPI (Vector Laboratories, CA, USA) for cell nuclei staining. The cells that invaded through the membranes were counted using the fluorescence microscope (Zeiss Axio Imager.Z1).

Immunohistochemistry (IHC)

Immunohistochemical staining of SDC4 was performed in accordance with previously described protocol (Magalhaes et al., 2009) on paraffin-embedded gastric carcinoma and lymph node sections. After deparaffination, rehydration and endogenous peroxidase blocking with 3% H_2O_2 diluted in methanol for 10 min, the sections were blocked with rabbit normal serum diluted in 10% BSA/PBS (1:5) for 30 min at room temperature. The serum solution was removed and sections were incubated with anti-SDC4 primary monoclonal antibody (8G3, (David et al., 1992)) diluted in 5% BSA/PBS (1:400) overnight at 4ºC. The slides were then washed twice in PBS-T (0.02%) and incubated for 30 min with biotinylated rabbit anti-mouse antibody (E0354, Dako, Glostrup, Denmark) diluted in 5%

BSA/PBS (1:200) at room temperature. Sections were washed twice in PBS-T (0.02%) and incubated with avidin–biotin complex (Vectastain Elite ABC kit, CA, USA) according to the manufacturer's recommendations for 30 min at room temperature. Staining was performed with 3,3'-diaminobenzidine tetrahydrochloride (Sigma-Aldrich®, MO,USA) containing 0.02% hydrogen peroxide. Slides were then counter-stained with Gill's hematoxylin (Bio Optica, Milan, Italy). Finally, the tissue sections were dehydrated and mounting medium (Thermo Fisher Scientific, MA, USA) was applied. Negative controls were performed by replacing the primary antibody with PBS. SDC4 expression was evaluated by an experienced pathologist, and the histological classification followed the Laurén guidelines (Lauren, 1965).

Statistical analysis

Statistical analyses were carried out using the online available GraphPad Prism software (GraphPad Software, Inc., CA, USA). The Student's t-test was performed to examine WB, qPCR, migration and invasion data. Fisher's exact test was used to examine the association between SDC4 expression and histological classification of gastric carcinomas. All p-values were considered significant when $p \leq 0.05$.

4. Results

Transient knockdown of SDC4

The transient knockdown of the SDC4 proteoglycan in AGS cell line was achieved by siRNA transfection which targets the SDC4 mRNA. The siRNA concentrations and the time points for protein extraction were optimized prior to the beginning of a set of silencing experiments. As a first step, each individual siRNA (A, B and C) and the combined formula (siRNA ABC) were tested at different concentrations (50nM and 100nM) in AGS cells. After 24h, 30h, 48h and 72h of siRNA transfection assay, a semi-quantitative analysis of SDC4 protein levels was done by WB.

As shown in Fig. 4.1, the individual siRNA B gave a percentage of transient silencing around 50%, but higher percentage of silencing was obtained combining the three individual siRNAs (near 80%).

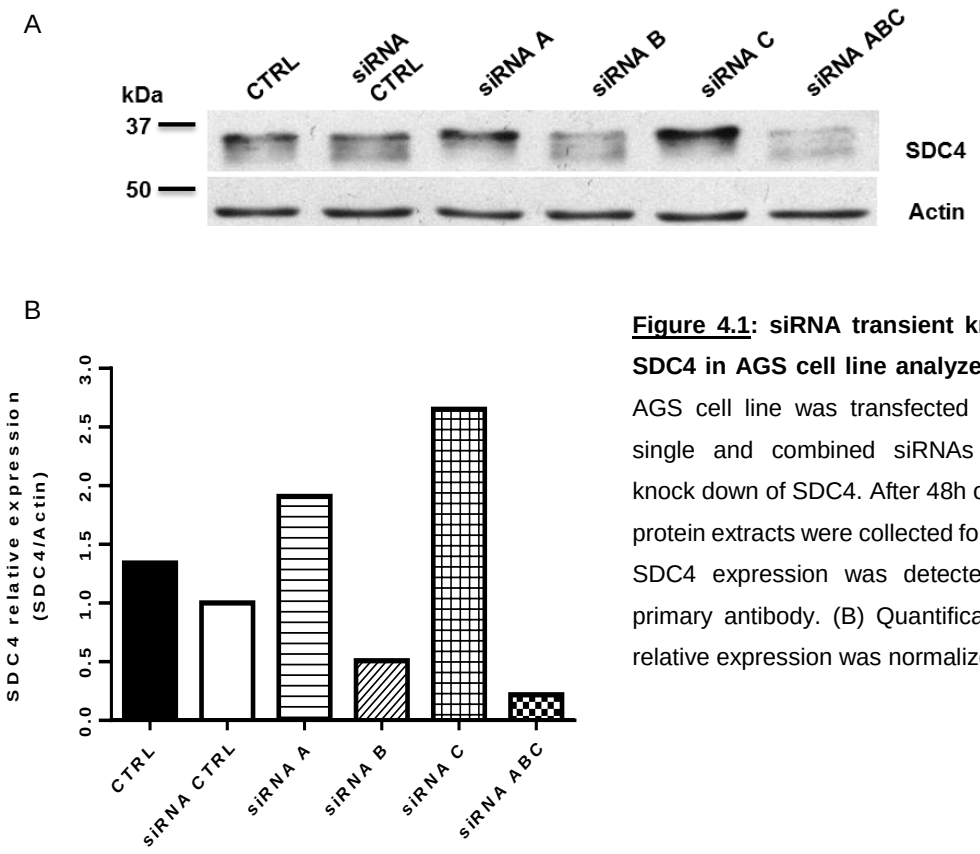

Figure 4.1: siRNA transient knockdown of SDC4 in AGS cell line analyzed by WB. (A) AGS cell line was transfected with 50nM of single and combined siRNAs for transient knock down of SDC4. After 48h of transfection, protein extracts were collected for WB analysis. SDC4 expression was detected using 5G9 primary antibody. (B) Quantification of SDC4 relative expression was normalized to actin.

This observation was confirmed by the use of two different primary antibodies (5G9 and H-140) raised against the extracellular domain of the SDC4 protein, through independent experiments (Fig. 4.2).

The combined siRNA ABC enables a transient silencing around 80% for SDC4 when compared to siRNA CTRL result (Fig. 4.2 A and B).This percentage was observed using the monoclonal 5G9 antibody, which detects a single SDC4 band. In contrast, the polyclonal H-140 antibody detects several bands, which can be due to variations of the glycosylation profile of SDC4. The percentage of SDC4 silencing according to H-140 antibody was around 50% (Fig. 4.2 C and D). This quantification is based on the sum of all bands shown for each lane, while 5G9 quantification relies on a single band detected. Based on these experiments, ideal conditions for SDC4 silencing were defined as concentration of 50nM for siRNA ABC and we observed that the peak of SDC4 transient silencing is reached after 48h of transfection.

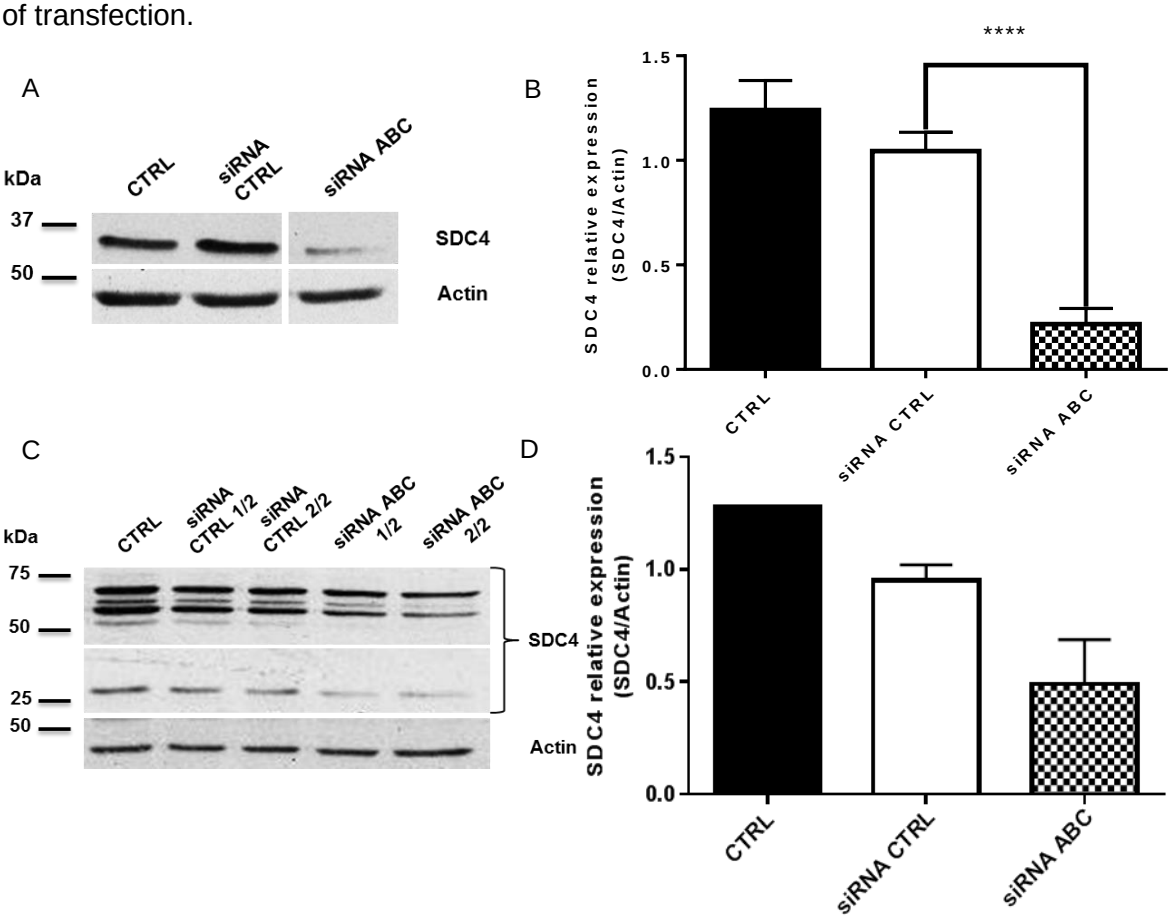

Figure 4.2: Transient knockdown of SDC4 in AGS cell line analyzed by WB. (A and C) AGS cell line was transfected with 50nM of siRNA CTRL and siRNA ABC for transient knock down of SDC4. After 48h of transfection, protein extracts were collected for WB analysis. SDC4 expression was detected using 5G9 (A) and H-140 (C) primary antibodies. (B and D) Quantification of SDC4 expression was normalized to actin. Results are described as Mean ± SD of three independent experiments (****p-value < 0.0001), and Mean ± SD for siRNA CTRL and siRNA ABC regarding duplicates in the same experiment, respectively.

To obtain a more accurate quantification of SDC4 transient silencing by siRNA transfection, RNA extracts were obtained in samples transfected with 50nM of siRNA ABC during 48h. A series of qPCR were performed to assess the content of SDC4 mRNA.

A high and constant percentage of SDC4 silencing was observed when the analysis was made by qPCR. The percentages of silencing observed were always around 80-85% through this quantitative method (Fig. 4.3). Therefore, we defined as silencing conditions transfecting the AGS cells with 50nM of siRNA ABC (siSDC4) for an established period of 48h.

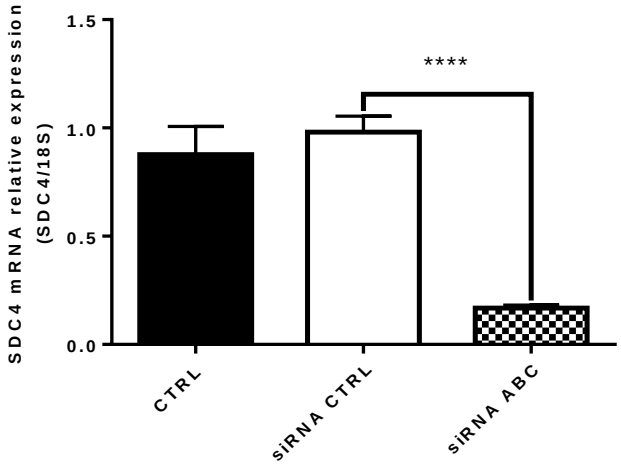

Figure 4.3: siRNA transient knockdown of SDC4 in AGS cell line analyzed by qPCR. AGS cell line was transfected with 50nM of siRNA CTRL and siRNA ABC for transient knockdown of SDC4. RNA was extracted 48h after transfection. Relative SDC4 expression levels of mRNA were measured by qPCR, and normalized to the expression level of 18S mRNA. Results are described as Mean ± SD of three independent experiments (****p-value < 0.0001).

Evaluation of SDC4 and β1 integrin expression upon SDC4 transient silencing

SDC4 and β1 integrin expression were evaluated by immunofluorescence analysis. As expected and in accordance with WB and qPCR data, it was observed a significant decrease in SDC4 expression upon SDC4 transient silencing. Variations in β1 integrin expression were observed when SDC4 is knocked down on AGS cells.

In siSDC4-transfected cells, the expression of β1 integrin is more restricted to the cell membrane compartment when compared with siCTRL-transfected and wild-type (WT) cells (Fig. 4.4).

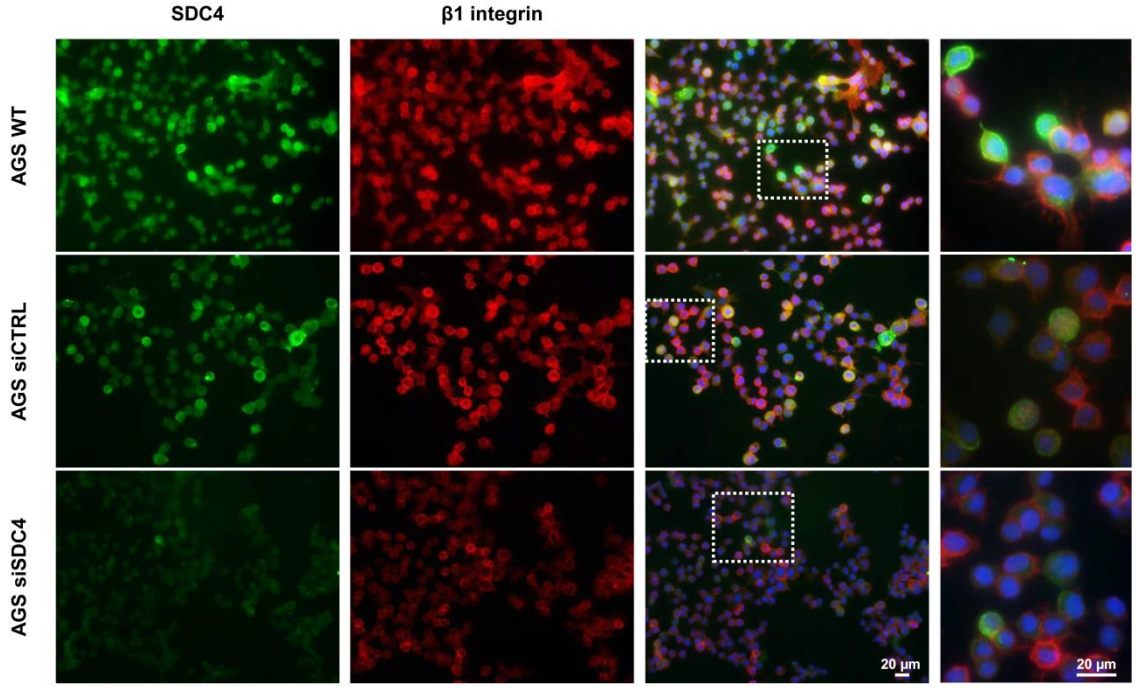

Figure 4.4: Double immunofluorescence of SDC4 and β1 integrin. AGS cell line after 48h of transfection with 50nM of siCTRL and siSDC4. The expression of SDC4 (5G9 antibody, in green) and β1 integrin (4B7R antibody, in red) was assessed under different conditions. Magnification of 200x and 630x (for the white outlined regions in the merged images).

To evaluate whether this effect was due to differences in β1 integrin expression levels, qPCRs were performed to assess the content of β1 integrin mRNA, using the RNA extracts obtained from the same SDC4 silencing experimental conditions. The expression levels of β1 integrin in siSDC4-transfected cells were identical to siCTRL-transfected cells (Fig. 4.5).

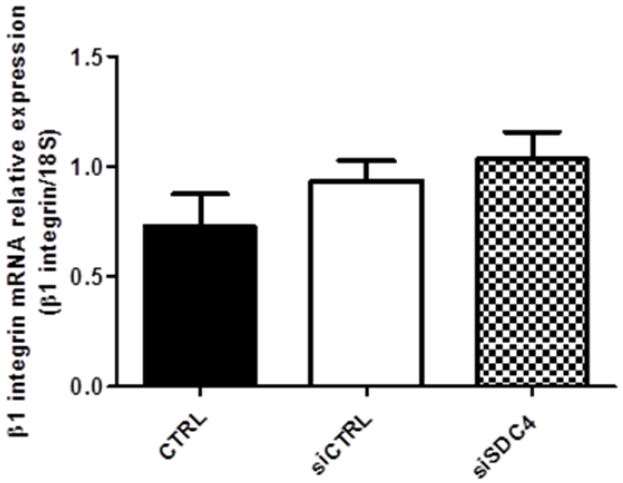

Figure 4.5: β1 integrin expression levels upon SDC4 transient silencing in AGS cell line analyzed by qPCR. AGS cell line was transfected with 50nM of siCTRL and siSDC4 for transient knockdown of SDC4. RNA was extracted 48h after transfection. Relative β1 integrin expression levels of mRNA were measured by qPCR, and normalized to the expression level of 18S mRNA. Results are described as Mean ± SD of two independent experiments.

We also observed that WT and siCTRL-transfected cells exhibit more membrane protrusions and an extended cellular morphology when compared to siSDC4-transfected cells, which present a more rounded morphology.

Evaluation of α-tubulin and actin expression upon SDC4 transient silencing

To better characterize cell morphology and formation of protrusive structures, the expression of α-tubulin and actin, two major components of the cell cytoskeleton, was analyzed by immunofluorescence analysis. The presence of protrusive and invasive structures, such as lamellipodia and filopodia, was very distinctive among the different AGS cell populations.

AGS cells silenced for SDC4 present rounded cell morphology and less formation of membrane protrusions compared to control populations. Both cytoskeleton proteins are limited to the membrane in SDC4 silenced cells, whereas a scattered distribution is observed in control cells (WT and siCTRL cells). Control cells exhibit protrusive structures with diverse spatial directions along the cell boundaries, with formation of lamellipodia and filopodia projections (Fig. 4.6).

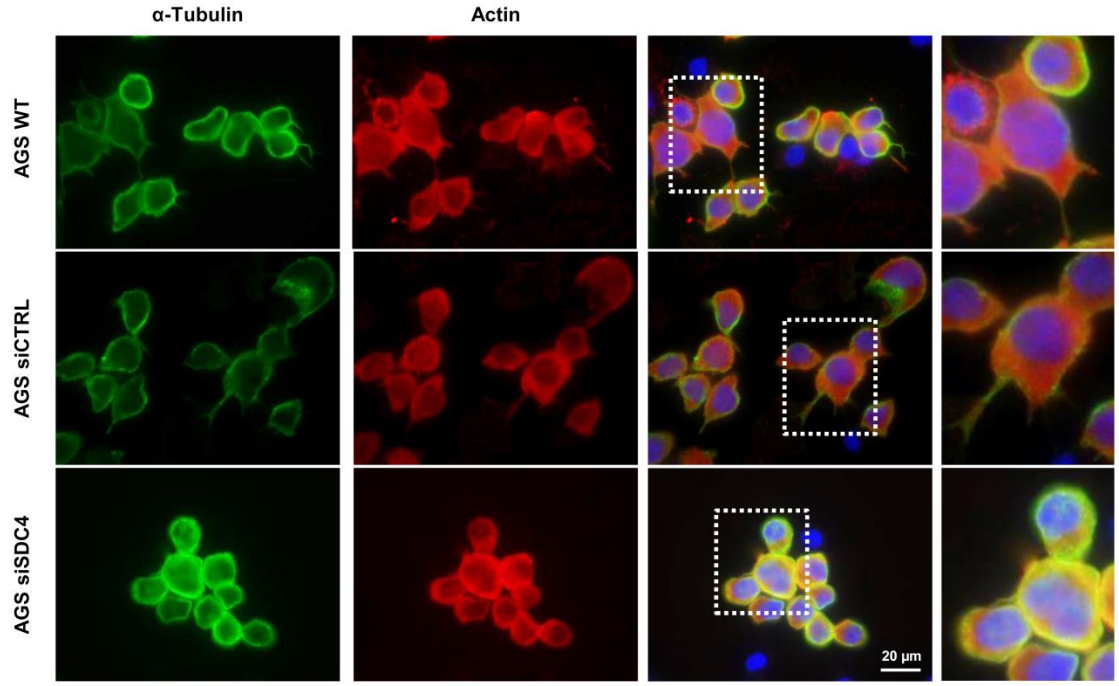

Figure 4.6: Double immunofluorescence of α-tubulin and actin. AGS cell line after 48h of transfection with 50nM of siCTRL and siSDC4. The expression of α-tubulin (T9026 antibody, in green) and actin (1616-R antibody, in red) was assessed under different conditions. The white outlined regions are represented with higher detail. Magnification of 630x.

Evaluation of SDC4 role in gastric cell migration

Knowing the key role of SDC4 in focal adhesion assembly, which directly influences cell motility, we decided to examine wether the SDC4 transient silencing influenced cell migration. To analyze cell migration capacity, cell exclusion zone assays were performed on siSDC4-transfected cells versus cells expressing normal levels of this proteoglycan.

In addition to changes in cytoskeletal patterning, both AGS transfected cell populations revealed differences in motile properties. The results showed that siSDC4-transfected cells migrated less compared to siCTRL-transfected cells (Fig 4.7 A). At the end of the 12h assay, the difference in migration percentage between both populations was 14% (Fig.4.7 B). The migration assay was performed after 36h of siRNA transfection and followed during 12h, coinciding with the 48h time point for SDC4 peak of transient silencing. To confirm that efficient SDC4 silencing was achieved, a qPCR was performed on both AGS cell populations that were siRNA transfected for performing the migration assay and a silencing percentage of 81% was achieved (Fig. 4.7 C), which is in accordance with previous qPCR results (Fig. 4.3).

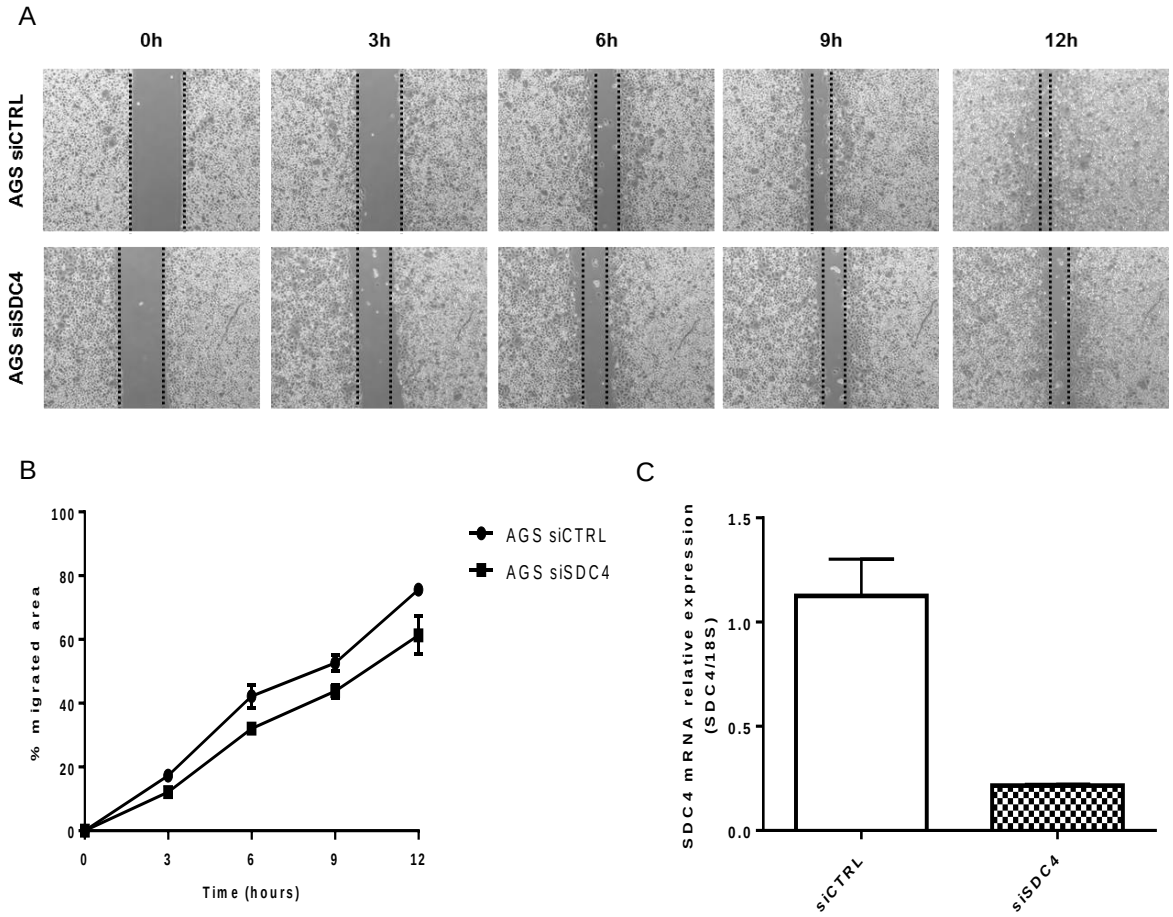

Figure 4.7: Migration assay. (A) Migration assay was performed after a siRNA transfection time-point of 36h. Cell migration was estimated by means of cell exclusion zone assay. The percentages of migrated areas were measured at every 3h, for a total period of 12h. (B) Percentage of migrated areas for both AGS cell populations represented as Mean ± SD for siCTRL and siSDC4 regarding duplicates in the same experiment. (C) After 48h of transfection, RNA extracts were collected for both AGS cell populations that were siRNA transfected for performing the migration assay. SDC4 mRNA relative expression levels were measured by qPCR and represented as Mean ± SD for siCTRL and siSDC4 regarding independent duplicates. The expression level of 18S mRNA was used for normalization of SDC4 mRNA relative expression levels.

Evaluation of SDC4 impact in gastric cell invasion

A 3D environment was used for analysis of SDC4 function regarding the invasion behavior of gastric cancer cells. The use of a gelatinous protein mixture commercialized as Matrigel (Hughes et al., 2010) is commonly used to mimic the ECM natural composition. To analyze gastric cell invasion, Matrigel coated transwells were used and siSDC4-transfected cells versus control cells were counted after 24h.

Knockdown of SDC4 yielded a more invasive phenotype compared to siCTRL-transfected cells (Fig. 4.8 A). The invasion assay was performed 24h after siRNA transfection. To assess the SDC4 silencing efficiency, qPCR was done using mRNA extracts from AGS cell populations that were siRNA transfected for performing the invasion assay after a 48h time point. The silencing percentage obtained (85%) (Fig. 4.8 B) is in agreement with all the previous qPCR results.

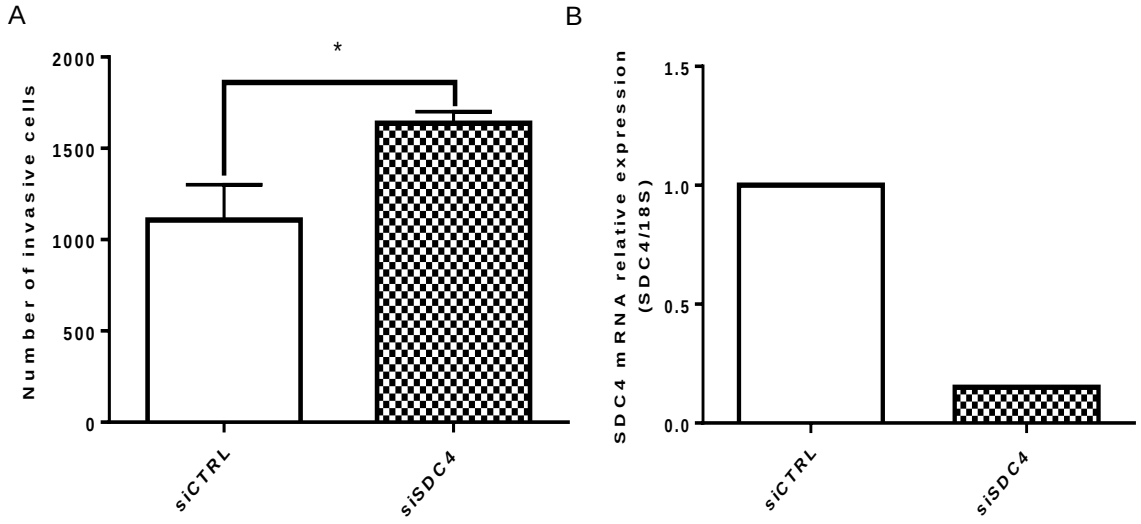

Figure 4.8: Invasion assay. (A) Invasion assay was performed after a siRNA transfection time-point of 24h. Cell Invasion was estimated by means of transwell invasion assay. After 24h of incubation in the transwells, the cells were stained with Vectashield with DAPI for counting. Independent triplicates for each AGS cell population (siCTRL and siSDC4) were done and invasive cells were counted. The average number of invasive cells are represented as Mean ± SD for siCTRL and siSDC4 regarding triplicates within the same experiment (*p-value=0.03). (B) After 48h of transfection, RNA extracts were collected for both AGS cell populations that were siRNA transfected for performing the invasion assay. SDC4 mRNA relative expression levels were measured by qPCR. The expression level of 18S mRNA was used for normalization of SDC4 mRNA relative expression levels.

Characterization of SDC4 expression in human gastric tumours

A set of 31 cases of gastric carcinomas were analyzed for SDC4 expression. Within this set, the three Laurén histological types of carcinomas: intestinal, diffuse and indeterminate were represented. The three histological types present a distinguished pattern for SDC4 expression within the neoplastic areas of the stomach. A set of 17 independent metastasis originated from the primary gastric carcinomas (previous set of gastric carcinomas) were also evaluated for SDC4 expression.

SDC4 staining was classified according to the extension and intensity of positivity. Non-neoplastic mucosa regions were negative for SDC4 staining (Fig. 4.9 A, images a and b). Most Intestinal-type carcinomas showed immunolabeling for SDC4 both in apical membrane and cytoplasmic areas of cells localized in glandular regions (Fig. 4.9 A, images c and d). Few Diffuse-type carcinomas displayed immunolabeling for SDC4 in cytoplasmic areas of isolated cells (Fig. 4.9 A, images e and f). The extension of SDC4 staining was grouped in two categories and a clear difference was observed (Fig. 4.9 B). Intestinal-type carcinomas presented a higher positivity for SDC4 in 65% of cases (n=11/17), while a lower positivity was observed in 35% of cases (n=6/17). Both diffuse and indeterminate carcinomas had the same pattern of extension, with low positivity in 86% of cases (n=6/7) and just 14% of high positivity in one case (n=1/7). A significant association was found between intestinal type carcinomas and SDC4 expression (p-value=0.028).

A

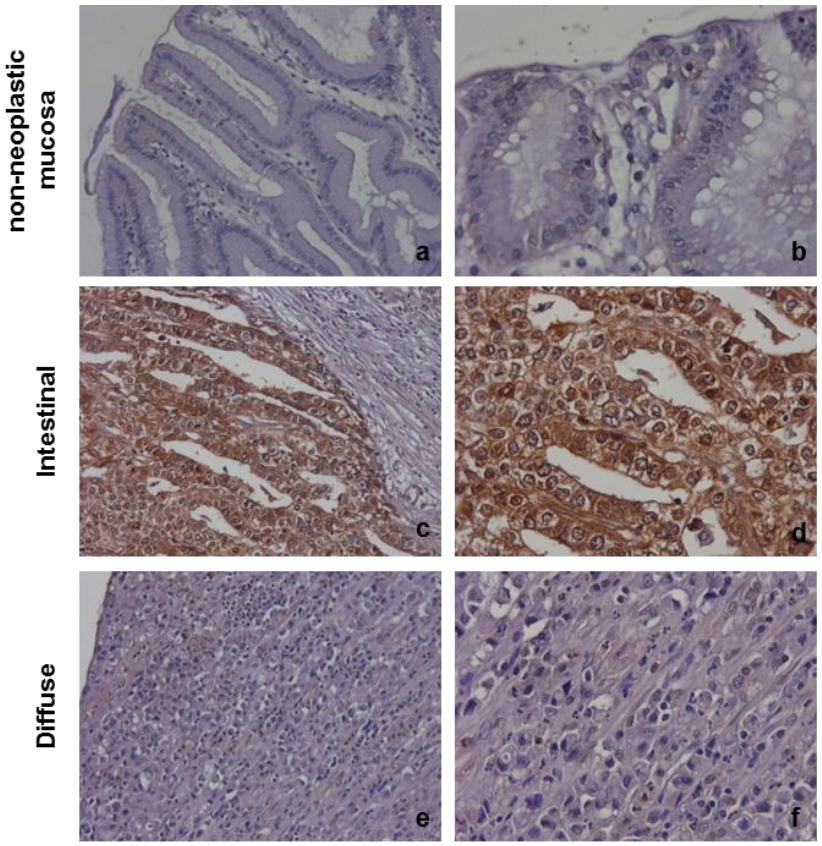

B

Figure 4.9: SDC4 expression in gastric primary carcinomas analyzed by IHC. (A) Non-neoplastic mucosa regions (a and b) and two main histological types of gastric carcinomas based on Laurén classification are represented: intestinal carcinoma (c and d) and diffuse carcinoma (e and f). SDC4 expression (brown staining) was detected using 8G3 primary antibody. Magnification of 200x for images a, c and e, and magnification of 400x for images b, d and f. (B) Percentage of SDC4 expression was assessed based on the extension and intensity of SDC4 staining (grouped in two categories: <25% - low positivity and weak intensity; >25% - high positivity and moderate or strong intensity). Intestinal carcinoma series is composed by 17 cases, while both indeterminate and diffuse carcinoma series are composed by 7 cases. Fisher's exact test: p-value=0,028.

Lymph node metastasis seems to follow the expression pattern of SDC4 observed in primary gastric carcinoma. SDC4 immunolabeling also exhibit the same pattern concerning subcellular areas (Fig. 4.10). Due to small series of metastasis for each histological type, statistical analysis cannot be performed.

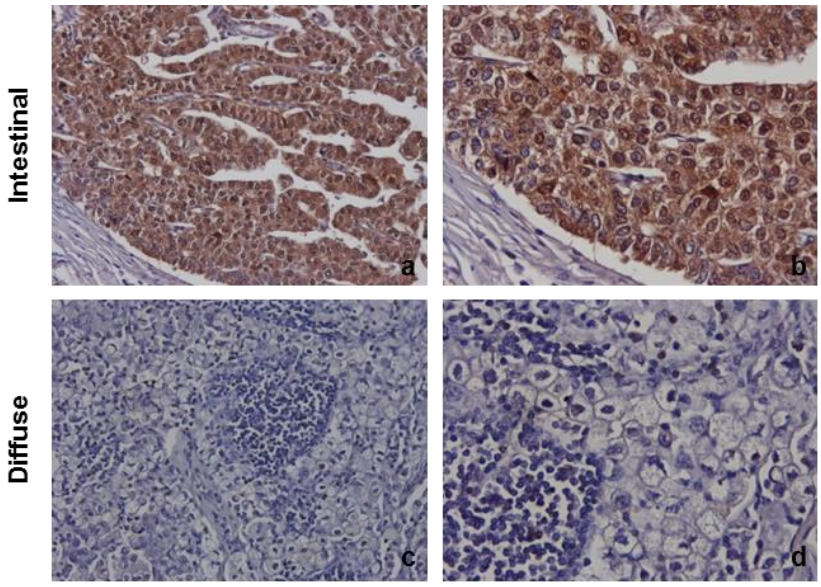

Figure 4.10: SDC4 expression in metastasis derived from primary gastric carcinomas analyzed by IHC. Lymph node metastasis derived from two main histological types of gastric primary carcinomas were used for SDC4 expression evaluation (brown staining), using 8G3 primary antibody. Magnification of 200x for images a and c, and magnification of 400x for images b and d.

5. Discussion

In the present work, it is demonstrated that SDC4 has important roles in major biological events during gastric carcinogenesis. Through an *in vitro* approach, an extensively used gastric cancer cell line was efficiently knocked down for SDC4 protein expression by siRNA transfection. This technique allowed not only to dissect the biological function of SDC4 in cell motility-based processes, but also to characterize the modulation of others cell membrane receptors expression. A shift in cell morphology and spatial distribution of cytoskeleton structural proteins, namely α-tubulin and actin, was noticed. The efficiency of transient SDC4 silencing was successfully high and stable by using a combination of three unique 27 mer siRNA duplexes (Fig. 4.1). In the first optimization steps, the silencing by transfection of each duplex alone could be excluded, even though the siRNA B induced a promising result. However, this observation was not reproduced in following experiments. These observations are in line with previous reports, since it has been described that siRNA duplexes alone frequently fail to considerably deplete their intended target, but increased numbers of duplexes rise the chance of generating the true loss-of-function phenotype for their specific target gene. This combination can translate the sum of partial knock-downs yielded by individual duplexes, giving rise to a more robust and detectable phenotype, when compared to phenotypes achieved by single transfected duplexes (Parsons et al., 2009). Another meaningful aspect is the time-point that produces a high value of transient silencing. The half-life of the protein encoded by the target gene can lead to misinterpreted results. Commonly, siRNAs induce a quick reduction of mRNA levels in ≤20h, but depletion of stable proteins is only achieved with longer time (Mocellin et al., 2006). When the rate of protein turnover is slow, even if the transcript levels are close to zero, sufficient amounts of protein can reside in the cell. Indeed, the variability observed when quantifying SDC4 at protein and mRNA levels can be justified by this proteoglycan half-life time. The usual HSPG half-life is 4-24h, with full turnover occurring at 48h (Knelson et al., 2014). The interpretation of siRNA transfection results by two distinctive methods, monitoring the SDC4 silencing not only at protein level (WB), but also at transcriptional level (qPCR), allowed to achieve more accurate outcomes. Using these two approaches, the transfection of a non-toxic concentration of siRNA ABC (50nM) over 48h on AGS cells yielded high rates of SDC4 transient silencing (around 80%) (Figs. 4.2 B and 4.3). These defined experimental conditions provided the best SDC4 silencing outcomes and therefore, were used in the following *in vitro* experiments.

The extensively studied association between SDC4 and integrins in the process of focal adhesion assembly encouraged the study of β1 integrin expression through immunofluorescence and qPCR analysis in the cells presenting reduced SDC4 levels. It was observed that in siSDC4-transfected cells, the β1 integrin was more confined to cell membrane (Fig. 4.4). SDC4 can act as an essential control point for integrin trafficking

directly promoting adhesion dynamics. It was shown that abrogation of SDC4 phosphorylation promotes surface expression of $\alpha_5\beta_1$ integrin and destabilization of the adhesion complexes (Morgan et al., 2013). Therefore, the presence of higher β1 integrin content in cell membrane can be explained by efficient SDC4 silencing, which prevents the initiation of phosphorylation events that could deeply influence the spatial distribution of β1 integrin. This higher membrane localization in siSDC4-transfected cells was not due to an increase on β1 integrin mRNA expression levels, which were assessed by qPCR using the same RNA extracts previously tested for SDC4 transient silencing evaluation (Fig. 4.5). These observations are in agreement with previous results showing that SDC4 WT cells and $SDC4^{-/-}$ cells express similar total levels of β1 integrin protein (Morgan et al., 2013). Together with this membrane receptor modulation, SDC4 can lead to cell morphology alterations that would affect cell behavior and interactions with ECM components. The analysis of cytoskeleton-associated α-tubulin and actin proteins expression allowed a better insight about overall cell morphology and the formation of protrusive structures, such as lamellipodia and filopodia. When SDC4 was transiently silenced, AGS cells showed a rounded morphology and a less extent of membrane protrusions when compared to both control population cells (Fig. 4.6). Similarly, a previous work showed that CHO-K1 cells transfected with wild-type SDC4 exhibit a more fibroblastic morphology, a greater degree of cell spreading and more salient microfilament bundles in contrast with cells presenting SDC4 truncated forms (Longley et al., 1999). Both SDC4 and β1 integrin are described has required for the rearrangement of the actin cytoskeleton into stress fibers (Okina et al., 2009). The membrane-proximal localization of tubulin and actin proteins was observed in siSD4-transfected cells, while in WT and siCTRL cells present a more scattered spatial disposition. It was shown previously that other minor cytoskeleton proteins, such as vinculin and paxillin, both assume peripheral expression in SDC4 null cells or in cells with some degree of SDC4 cytoplasmic domain truncation (Longley et al., 1999, Midwood et al., 2004). Formation of protrusive structures is dependent on parallel regulation of multiple GTPases that can be successfully accomplished between the engagement of both SDC4 and integrins. The observation of less lamellipodia and filopodia formation in siSDC4-transfected cells shows that knockdown of SDC4 alone largely affects the development of such structures and therefore impacts cell morphology.

Cell motility can be directly regulated by the interactions between membrane receptors and the ECM. The described upregulation of SDC4 in wound repair processes (Gallo et al., 1996) demonstrates the importance of this proteoglycan for key carcinogenic events, such as migration and invasion. Less migration ability was observed for siSDC4-transfected cells when compared to siCTRL-transfected cells, although the difference in migrated area percentage was just 14% (Fig.4.7 A and B). This small difference in migration

capacity can be justified by the use of uncoated plastic surfaces. Previous studies have shown that uncoated surfaces do not substantially change the migration rates of cells transfected with various SDC4 constructs, in contrast with fibronectin and vitronectin substrates used on parallel experiments (Longley et al., 1999). Similarly to our observation, using a mouse model where SDC4 gene was disrupted, $SDC4^{-/-}$ fibroblasts showed delayed migration when compared to WT fibroblasts by a wound healing repair assay (Echtermeyer et al., 2001) Because SDCs act as receptors for both insoluble ligands composing the ECM and soluble ligands such as growth factors, the observed delay in SDC4-silenced AGS cells could result from an impairment of either or both of these functions. Regarding the invasion assay in a substrate mimicking the ECM, SDC4-silenced cells showed higher invasion capacity (Fig 4.8 A). This is in agreement with previous results, showing that SDC4 silencing increased invasion in a breast cancer cell line (Vuoriluoto et al., 2011). In this previous study, the cells appeared to migrate collectively like strand patterns, instead of isolated cells (Vuoriluoto et al., 2011). SDC4 negative role in invasion regulation in gastric cancer cells can be guided by the cooperative engagement of SDC4 and α5β1 integrin, since both receptors influence cell motility and contractility within 3D matrix through focal adhesion assembly and stress fibers formation (Midwood et al., 2004). Taking migration and invasion assays into consideration, the signaling events controlling cell adhesions can be different between the 2D and 3D models (Cukierman et al., 2002, Midwood et al., 2004)

Syndecans have been suggested to be used as biomarkers and prognostic factors for a variety of tumour types, since they are involved in main processes regarding cancer progression. Aberrant expression of SDC4 was reported in breast cancer, hepatocellular carcinoma, melanoma and malignant mesothelioma (Couchman et al., 2015), although so far few studies have examined the critical role of SDC4 in gastric malignancy. It was previously reported that highly pathogenic *H. pylori* strains induce SDC4 expression in human gastric mucosas (Magalhaes et al., 2009). Since there was no data concerning SDC4 expression in malignant gastric tissues, an immunohistological approach was used to evaluate SDC4 in gastric tumour. SDC4 expression was evaluated concerning three histological types of primary gastric cancers. Non-neoplastic mucosa regions did not present SDC4 staining (Fig. 4.9 A, images a and b). A higher expression of SDC4 was evident in intestinal-type carcinomas and SDC4 labelling was present in both apical membrane and cytoplasmic areas (Fig.4.9 A, images c and d). Intestinal-type series showed 65% of SDC4 high positivity (Fig. 4.9 B). The higher rate of positivity for SDC4 is significantly associated to a type of gastric carcinoma that progresses through a series of well-defined histological steps. This association can underlie a possible SDC4 role in the establishment of gastric carcinogenesis that may be related with *H. pylori* infection. Since *H. pylori* can increase the expression of SDC4 (Smith et al., 2006, Magalhaes et al., 2009), this

membrane receptor could be targeted for gastric therapeutic approaches. Lower positivity was observed in both diffuse and indeterminate carcinomas (Fig. 4.9 B). The few SDC4 stained cells displayed SDC4 labelling restricted to cytoplasm (Fig. 4.9 A, images e and f). Absence of SDC4 expression in these histological type carcinomas can induce the poorly cohesive cells to reach a more profound infiltration trough the stomach wall. Interestingly, it was demonstrated that loss of SDC1 is often associated with loss of E-cadherin (Iozzo and Sanderson, 2011). The evolution of diffuse gastric carcinomas is strongly associated with loss of E-cadherin (Graziano et al., 2003), so together with the loss of SDC4, it can propel cells to epithelial to mesenchymal transition. It was observed that lymph node metastasis derived from both intestinal and diffuse primary carcinomas followed the same trend, regarding SDC4 expression and localization in cells (Fig. 4.10).

6. Final conclusions

The results obtained in this work highlight the importance of SDC4 proteoglycan in gastric carcinogenesis. A transient silencing technique through siRNA transfection allowed the analysis of SDC4 functions, namely in the modulation of expression and spatial distribution of other receptors and in cell morphology and motility mechanisms. SDC4 directly influences the expression and trafficking of β1 integrin to the membrane, which emphasizes their cooperative modulation for multiple signaling events that initiate at the membrane. Cell morphology changes are dependent of SDC4 expression, which has a direct impact in the overall cell shape and in the formation of membrane-associated structures, such as lamellipodia and filopodia. Cell motility experiments showed that SDC4 can directly influence the motility capacity of gastric cancer cells, giving them less migratory ability but higher invasiveness when it is transiently absent.

SDC4 expression was also evaluated on malignant gastric tissues and we observed that its expression is associated with the histological type of gastric primary carcinomas. Intestinal-type carcinomas showed higher expression of SDC4 when compared with both diffuse and indeterminate carcinomas, and its cellular localization at the membrane can reveal a possible role for gastric carcinogenesis progress. SDC4 labelling in lymph node metastasis followed the same trend as the respective primary carcinomas.

Altogether, our results have contributed to characterize the functional role of SDC4 in modulating gastric cancer cell behaviour. Moreover, this study sets the ground to further evaluate SDC4 as a possible gastric cancer biomarker and as a novel target for therapeutical intervention.

7. Future perspectives

The set of results previously presented reinforce the wide action spectrum that proteoglycans, namely SDCs, can have during tumourigenesis processes. The disease model studied on this work was gastric cancer since it lacked information regarding SDC4 expression and biological functions. Additional studies are necessary in order to further characterize the role of SDC4 in gastric cancer cell biology and to validate our observations.

Thus, we intend to perform fluorescence-activated cell sorting (FACS) analysis to quantify SDC4 and β1 integrin expression levels at the cell membrane. Proximity ligation assays (PLA) should also be done to assess in detail the co-expression trend of both membrane receptors, considering the interactions of gastric cells with different ECM proteins, such as fibronectin and collagen.

Migration assays performed with uncoated surfaces did not show significant variations between SDC4 silenced cells and control cells. Therefore, it would be of interest to assess the migration ability of SDC4-silenced cells considering different coatings (fibronectin and collagen).

Since both membrane receptors, integrins and SDCs, act cooperatively for the regulation of multiple GTPases, a pull down assay to determine their activation regarding SDC4 transient silencing could help to explain their putative involvement in altered gastric cell morphology and motility.

Finally, evaluation of SDC4 expression in a larger series of human gastric carcinoma and metastasis samples would strengthen the statistical analysis and would help to delineate a distinct profile of SDC4 expression concerning the three Laurén histological types of gastric carcinomas and support its application as a putative gastric cancer biomarker.

8. References

Apweiler R, Hermjakob H, Sharon N (1999) On the frequency of protein glycosylation, as deduced from analysis of the SWISS-PROT database. Biochim Biophys Acta 1473:4-8.

Atherton JC (2006) The pathogenesis of Helicobacter pylori-induced gastro-duodenal diseases. Annu Rev Pathol 1:63-96.

Barbouri D, Afratis N, Gialeli C, Vynios DH, Theocharis AD, Karamanos NK (2014) Syndecans as modulators and potential pharmacological targets in cancer progression. Front Oncol 4:4.

Barczyk M, Carracedo S, Gullberg D (2010) Integrins. Cell Tissue Res 339:269-280.

Barranco SC, Townsend CM, Jr., Casartelli C, Macik BG, Burger NL, Boerwinkle WR, Gourley WK (1983) Establishment and characterization of an in vitro model system for human adenocarcinoma of the stomach. Cancer Res 43:1703-1709.

Bass MD, Morgan MR, Humphries MJ (2007) Integrins and syndecan-4 make distinct, but critical, contributions to adhesion contact formation. Soft Matter 3:372-376.

Beauvais DM, Rapraeger AC (2004) Syndecans in tumor cell adhesion and signaling. Reprod Biol Endocrinol 2:3.

Berlth F, Bollschweiler E, Drebber U, Hoelscher AH, Moenig S (2014) Pathohistological classification systems in gastric cancer: diagnostic relevance and prognostic value. World J Gastroenterol 20:5679-5684.

Bertozzi CR, D R (2009) Structural Basis of Glycan Diversity. In: Essentials of Glycobiology (Varki, A. et al., eds) Cold Spring Harbor (NY): Cold Spring Harbor Laboratory Press.

Bhandari A, Crowe SE (2012) Helicobacter pylori in gastric malignancies. Curr Gastroenterol Rep 14:489-496.

Bouvard D, Brakebusch C, Gustafsson E, Aszodi A, Bengtsson T, Berna A, Fassler R (2001) Functional consequences of integrin gene mutations in mice. Circ Res 89:211-223.

Brooks R, Williamson R, Bass M (2012) Syndecan-4 independently regulates multiple small GTPases to promote fibroblast migration during wound healing. Small GTPases 3:73-79.

Caffaro CE, Hirschberg CB, Berninsone PM (2006) Independent and simultaneous translocation of two substrates by a nucleotide sugar transporter. Proc Natl Acad Sci U S A 103:16176-16181.

Caramelo JJ, Parodi AJ (2007) How sugars convey information on protein conformation in the endoplasmic reticulum. Semin Cell Dev Biol 18:732-742.

Carlsson P, Presto J, Spillmann D, Lindahl U, Kjellen L (2008) Heparin/heparan sulfate biosynthesis: processive formation of N-sulfated domains. J Biol Chem 283:20008-20014.

Chen RL, Lander AD (2001) Mechanisms underlying preferential assembly of heparan sulfate on glypican-1. J Biol Chem 276:7507-7517.

Choi Y, Chung H, Jung H, Couchman JR, Oh ES (2011) Syndecans as cell surface receptors: Unique structure equates with functional diversity. Matrix Biol 30:93-99.

Chomczynski P (1993) A reagent for the single-step simultaneous isolation of RNA, DNA and proteins from cell and tissue samples. Biotechniques 15:532-534, 536-537.

Christiansen MN, Chik J, Lee L, Anugraham M, Abrahams JL, Packer NH (2014) Cell surface protein glycosylation in cancer. Proteomics 14:525-546.

Correa P (1992) Human gastric carcinogenesis: a multistep and multifactorial process--First American Cancer Society Award Lecture on Cancer Epidemiology and Prevention. Cancer Res 52:6735-6740.

Couchman JR (2010) Transmembrane signaling proteoglycans. Annu Rev Cell Dev Biol 26:89-114.

Couchman JR, Gopal S, Lim HC, Norgaard S, Multhaupt HA (2015) Syndecans: from peripheral coreceptors to mainstream regulators of cell behaviour. Int J Exp Pathol 96:1-10.

Couchman JR, Pataki CA (2012) An introduction to proteoglycans and their localization. J Histochem Cytochem 60:885-897.

Cukierman E, Pankov R, Yamada KM (2002) Cell interactions with three-dimensional matrices. Curr Opin Cell Biol 14:633-639.

David G, van der Schueren B, Marynen P, Cassiman JJ, van den Berghe H (1992) Molecular cloning of amphiglycan, a novel integral membrane heparan sulfate proteoglycan expressed by epithelial and fibroblastic cells. J Cell Biol 118:961-969.

DeMali KA, Wennerberg K, Burridge K (2003) Integrin signaling to the actin cytoskeleton. Curr Opin Cell Biol 15:572-582.

Dicken BJ, Bigam DL, Cass C, Mackey JR, Joy AA, Hamilton SM (2005) Gastric adenocarcinoma: review and considerations for future directions. Ann Surg 241:27-39.

Echtermeyer F, Streit M, Wilcox-Adelman S, Saoncella S, Denhez F, Detmar M, Goetinck P (2001) Delayed wound repair and impaired angiogenesis in mice lacking syndecan-4. J Clin Invest 107:R9-R14.

Edwards IJ (2012) Proteoglycans in prostate cancer. Nat Rev Urol 9:196-206.

Elfenbein A, Simons M (2013) Syndecan-4 signaling at a glance. J Cell Sci 126:3799-3804.

Esko JD, Kimata K, Lindahl U (2009) Proteoglycans and sulfated glycosaminoglycans. In: Essentials of Glycobiology, vol. 2nd Edition (Varki, A. et al., eds), p Chapter 16 Cold Spring Harbor (NY)

Ferlay J, Shin HR, Bray F, Forman D, Mathers C, Parkin DM (2010) Estimates of worldwide burden of cancer in 2008: GLOBOCAN 2008. Int J Cancer 127:2893-2917.

Ferlay J, Soerjomataram I, Dikshit R, Eser S, Mathers C, Rebelo M, Parkin DM, Forman D, Bray F (2015) Cancer incidence and mortality worldwide: sources, methods and major patterns in GLOBOCAN 2012. Int J Cancer 136:E359-386.

Ferronha I, Castro C, Carreira H, Bento MJ, Carvalho I, Peleteiro B, Lunet N (2012) Prediagnosis lifestyle exposures and survival of gastric cancer patients: a cohort study from Portugal. Br J Cancer 107:537-543.

Fuster MM, Esko JD (2005) The sweet and sour of cancer: glycans as novel therapeutic targets. Nat Rev Cancer 5:526-542.

Gallagher JT (2001) Heparan sulfate: growth control with a restricted sequence menu. J Clin Invest 108:357-361.

Gallo R, Kim C, Kokenyesi R, Adzick NS, Bernfield M (1996) Syndecans-1 and -4 are induced during wound repair of neonatal but not fetal skin. J Invest Dermatol 107:676-683.

Gandhi NS, Mancera RL (2008) The structure of glycosaminoglycans and their interactions with proteins. Chem Biol Drug Des 72:455-482.

Graziano F, Humar B, Guilford P (2003) The role of the E-cadherin gene (CDH1) in diffuse gastric cancer susceptibility: from the laboratory to clinical practice. Ann Oncol 14:1705-1713.

Haj-Sheykholeslami A, Rakhshani N, Amirzargar A, Rafiee R, Shahidi SM, Nikbin B, Khosravi F, Massarrat S (2008) Serum pepsinogen I, pepsinogen II, and gastrin 17 in relatives of gastric cancer patients: comparative study with type and severity of gastritis. Clin Gastroenterol Hepatol 6:174-179.

Hu B, El Hajj N, Sittler S, Lammert N, Barnes R, Meloni-Ehrig A (2012) Gastric cancer: Classification, histology and application of molecular pathology. J Gastrointest Oncol 3:251-261.

Hughes CS, Postovit LM, Lajoie GA (2010) Matrigel: a complex protein mixture required for optimal growth of cell culture. Proteomics 10:1886-1890.

Humphries JD, Byron A, Humphries MJ (2006) Integrin ligands at a glance. J Cell Sci 119:3901-3903.

IARC (1994) Schistosomes, liver flukes and Helicobacter pylori. IARC Working Group on the Evaluation of Carcinogenic Risks to Humans. Lyon, 7-14 June 1994. IARC Monogr Eval Carcinog Risks Hum 61:1-241.

Iozzo RV, Sanderson RD (2011) Proteoglycans in cancer biology, tumour microenvironment and angiogenesis. J Cell Mol Med 15:1013-1031.

Kamangar F, Dawsey SM, Blaser MJ, Perez-Perez GI, Pietinen P, Newschaffer CJ, Abnet CC, Albanes D, Virtamo J, Taylor PR (2006) Opposing risks of gastric cardia and noncardia gastric adenocarcinomas associated with Helicobacter pylori seropositivity. J Natl Cancer Inst 98:1445-1452.

Kato M, Asaka M (2012) Recent development of gastric cancer prevention. Jpn J Clin Oncol 42:987-994.

Kato M, Wang H, Bernfield M, Gallagher JT, Turnbull JE (1994) Cell surface syndecan-1 on distinct cell types differs in fine structure and ligand binding of its heparan sulfate chains. J Biol Chem 269:18881-18890.

Knelson EH, Nee JC, Blobe GC (2014) Heparan sulfate signaling in cancer. Trends Biochem Sci 39:277-288.

Kreuger J, Kjellen L (2012) Heparan sulfate biosynthesis: regulation and variability. J Histochem Cytochem 60:898-907.

Lambaerts K, Wilcox-Adelman SA, Zimmermann P (2009) The signaling mechanisms of syndecan heparan sulfate proteoglycans. Curr Opin Cell Biol 21:662-669.

Lauren P (1965) The Two Histological Main Types of Gastric Carcinoma: Diffuse and So-Called Intestinal-Type Carcinoma. An Attempt at a Histo-Clinical Classification. Acta Pathol Microbiol Scand 64:31-49.

Li Q, Zhang J, Zhou Y, Qiao L (2012) Obesity and gastric cancer. Front Biosci (Landmark Ed) 17:2383-2390.

Lidholt K, Lindahl U (1992) Biosynthesis of heparin. The D-glucuronosyl- and N-acetyl-D-glucosaminyltransferase reactions and their relation to polymer modification. Biochem J 287 (Pt 1):21-29.

Lin F, Ren XD, Doris G, Clark RA (2005) Three-dimensional migration of human adult dermal fibroblasts from collagen lattices into fibrin/fibronectin gels requires syndecan-4 proteoglycan. J Invest Dermatol 124:906-913.

Longley RL, Woods A, Fleetwood A, Cowling GJ, Gallagher JT, Couchman JR (1999) Control of morphology, cytoskeleton and migration by syndecan-4. J Cell Sci 112 (Pt 20):3421-3431.

Lu B, Li M (2014) Helicobacter pylori eradication for preventing gastric cancer. World Journal of Gastroenterology : WJG 20:5660-5665.

Machesky LM (2008) Lamellipodia and filopodia in metastasis and invasion. FEBS Lett 582:2102-2111.

Magalhaes A, Marcos-Pinto R, Nairn AV, Dela Rosa M, Ferreira RM, Junqueira-Neto S, Freitas D, Gomes J, Oliveira P, Santos MR, Marcos NT, Xiaogang W, Figueiredo C, Oliveira C, Dinis-Ribeiro M, Carneiro F, Moremen KW, David L, Reis CA (2015) Helicobacter pylori chronic infection and mucosal inflammation switches the human gastric glycosylation pathways. Biochim Biophys Acta 1852:1928-1939.

Magalhaes A, Marcos NT, Carvalho AS, David L, Figueiredo C, Bastos J, David G, Reis CA (2009) Helicobacter pylori cag pathogenicity island-positive strains induce syndecan-4 expression in gastric epithelial cells. FEMS Immunol Med Microbiol 56:223-232.

Magalhaes A, Reis CA (2010) Helicobacter pylori adhesion to gastric epithelial cells is mediated by glycan receptors. Braz J Med Biol Res 43:611-618.

Manon-Jensen T, Itoh Y, Couchman JR (2010) Proteoglycans in health and disease: the multiple roles of syndecan shedding. FEBS J 277:3876-3889.

Massarrat S, Stolte M (2014) Development of gastric cancer and its prevention. Arch Iran Med 17:514-520.

Matsuoka T, Yashiro M (2014) Rho/ROCK signaling in motility and metastasis of gastric cancer. World J Gastroenterol 20:13756-13766.

Mera R, Fontham ET, Bravo LE, Bravo JC, Piazuelo MB, Camargo MC, Correa P (2005) Long term follow up of patients treated for Helicobacter pylori infection. Gut 54:1536-1540.

Midwood KS, Valenick LV, Hsia HC, Schwarzbauer JE (2004) Coregulation of fibronectin signaling and matrix contraction by tenascin-C and syndecan-4. Mol Biol Cell 15:5670-5677.

Mocellin S, Costa R, Nitti D (2006) RNA interference: ready to silence cancer? J Mol Med (Berl) 84:4-15.

Montreuil J (1980) Primary structure of glycoprotein glycans: basis for the molecular biology of glycoproteins. Adv Carbohydr Chem Biochem 37:157-223.

Morgan MR, Hamidi H, Bass MD, Warwood S, Ballestrem C, Humphries MJ (2013) Syndecan-4 phosphorylation is a control point for integrin recycling. Dev Cell 24:472-485.

Morgan MR, Humphries MJ, Bass MD (2007) Synergistic control of cell adhesion by integrins and syndecans. Nat Rev Mol Cell Biol 8:957-969.

Multhaupt HA, Yoneda A, Whiteford JR, Oh ES, Lee W, Couchman JR (2009) Syndecan signaling: when, where and why? J Physiol Pharmacol 60 Suppl 4:31-38.

Nugent MA, Zaia J, Spencer JL (2013) Heparan sulfate-protein binding specificity. Biochemistry (Mosc) 78:726-735.

Oh ES, Woods A, Lim ST, Theibert AW, Couchman JR (1998) Syndecan-4 proteoglycan cytoplasmic domain and phosphatidylinositol 4,5-bisphosphate coordinately regulate protein kinase C activity. J Biol Chem 273:10624-10629.

Ohtsubo K, Marth JD (2006) Glycosylation in cellular mechanisms of health and disease. Cell 126:855-867.

Okina E, Manon-Jensen T, Whiteford JR, Couchman JR (2009) Syndecan proteoglycan contributions to cytoskeletal organization and contractility. Scand J Med Sci Sports 19:479-489.

Pandey R, Misra V, Misra SP, Dwivedi M, Kumar A, Tiwari BK (2010) Helicobacter pylori and gastric cancer. Asian Pac J Cancer Prev 11:583-588.

Parsons BD, Schindler A, Evans DH, Foley E (2009) A direct phenotypic comparison of siRNA pools and multiple individual duplexes in a functional assay. PLoS One 4:e8471.

Piazuelo MB, Correa P (2013) Gastric cancer: Overview. Colomb Med (Cali) 44:192-201.

Pinheiro H, Oliveira C, Seruca R, Carneiro F (2014) Hereditary diffuse gastric cancer - pathophysiology and clinical management. Best Pract Res Clin Gastroenterol 28:1055-1068.

Pinho SS, Carvalho S, Marcos-Pinto R, Magalhaes A, Oliveira C, Gu J, Dinis-Ribeiro M, Carneiro F, Seruca R, Reis CA (2013) Gastric cancer: adding glycosylation to the equation. Trends Mol Med 19:664-676.

Pinho SS, Reis CA (2015) Glycosylation in cancer: mechanisms and clinical implications. Nat Rev Cancer 15:540-555.

Rapraeger A, Jalkanen M, Endo E, Koda J, Bernfield M (1985) The cell surface proteoglycan from mouse mammary epithelial cells bears chondroitin sulfate and heparan sulfate glycosaminoglycans. J Biol Chem 260:11046-11052.

Reis CA, David L, Correa P, Carneiro F, de Bolos C, Garcia E, Mandel U, Clausen H, Sobrinho-Simoes M (1999) Intestinal metaplasia of human stomach displays distinct patterns of mucin (MUC1, MUC2, MUC5AC, and MUC6) expression. Cancer Res 59:1003-1007.

Reis CA, Osorio H, Silva L, Gomes C, David L (2010) Alterations in glycosylation as biomarkers for cancer detection. J Clin Pathol 63:322-329.

Resende C, Ristimaki A, Machado JC (2010) Genetic and epigenetic alteration in gastric carcinogenesis. Helicobacter 15 Suppl 1:34-39.

Roper JA, Williamson RC, Bass MD (2012) Syndecan and integrin interactomes: large complexes in small spaces. Curr Opin Struct Biol 22:583-590.

Rudd TR, Yates EA (2012) A highly efficient tree structure for the biosynthesis of heparan sulfate accounts for the commonly observed disaccharides and suggests a mechanism for domain synthesis. Mol Biosyst 8:1499-1506.

Sarrazin S, Lamanna WC, Esko JD (2011) Heparan sulfate proteoglycans. Cold Spring Harb Perspect Biol 3.

Schaefer L, Schaefer RM (2010) Proteoglycans: from structural compounds to signaling molecules. Cell Tissue Res 339:237-246.

Shi J, Qu YP, Hou P (2014) Pathogenetic mechanisms in gastric cancer. World J Gastroenterol 20:13804-13819.

Smith MF, Jr., Novotny J, Carl VS, Comeau LD (2006) Helicobacter pylori and toll-like receptor agonists induce syndecan-4 expression in an NF-kappaB-dependent manner. Glycobiology 16:221-229.

Spiro RG (2002) Protein glycosylation: nature, distribution, enzymatic formation, and disease implications of glycopeptide bonds. Glycobiology 12:43r-56r.

Stowell SR, Ju T, Cummings RD (2015) Protein glycosylation in cancer. Annu Rev Pathol 10:473-510.

Szatmari T, Dobra K (2013) The role of syndecan-1 in cellular signaling and its effects on heparan sulfate biosynthesis in mesenchymal tumors. Front Oncol 3:310.

Theocharis AD, Skandalis SS, Tzanakakis GN, Karamanos NK (2010) Proteoglycans in health and disease: novel roles for proteoglycans in malignancy and their pharmacological targeting. Febs j 277:3904-3923.

Tkachenko E, Rhodes JM, Simons M (2005) Syndecans: new kids on the signaling block. Circ Res 96:488-500.

Tuccillo FM, de Laurentiis A, Palmieri C (2014) Aberrant glycosylation as biomarker for cancer: focus on CD43. 2014:742831.

Vuoriluoto K, Hognas G, Meller P, Lehti K, Ivaska J (2011) Syndecan-1 and -4 differentially regulate oncogenic K-ras dependent cell invasion into collagen through alpha2beta1 integrin and MT1-MMP. Matrix Biol 30:207-217.

Wang F, Meng W, Wang B, Qiao L (2014) Helicobacter pylori-induced gastric inflammation and gastric cancer. Cancer Lett 345:196-202.

Woods A, Couchman JR (2001) Syndecan-4 and focal adhesion function. Curr Opin Cell Biol 13:578-583.

Wroblewski LE, Peek RM, Jr., Wilson KT (2010) Helicobacter pylori and gastric cancer: factors that modulate disease risk. Clin Microbiol Rev 23:713-739.

Xiong S, Zhang L, He QY (2008) Fractionation of proteins by heparin chromatography. Methods Mol Biol 424:213-221.